ISSN 2523-2517

Volume 7, Issue 19 – July – December – 2023

Journal Electrical Engineering

ECORFAN®

Journal Electrical Engineering, Volume 7, Issue 19, December, 2023, is a magazine published biannually by ECORFAN-Peru. La Raza Av. 1047 No. - Santa Ana, CuscoPeru. Postcode: 11500. WEB: www.ecorfan.org/republicofperu, revista@ecorfan.org. Editor in Chief: QUINTANILLA - CÓNDOR, Cerapio. PhD. ISSN: 2523-2517. Responsible for the last update of this issue of the ECORFAN Informatics Unit. ESCAMILLA-BOUCHÁN Imelda, LUNA-SOTO, Vladimir, updated December 31, 2023.

Journal Electrical Engineering

Definition of Journal

Scientific Objectives

Support the international scientific community in its written production Science, Technology and Innovation in the Field of Engineering and Technology, in Subdisciplines Electromagnetism, electrical distribution sources, electrical engineering innovation, signal amplification, electric motor design, material science in power plants, management and distribution of electrical energies.

ECORFAN-Mexico, S.C. is a Scientific and Technological Company in contribution to the Human Resource training focused on the continuity in the critical analysis of International Research and is attached to CONAHCYT-RENIECYT number 1702902, its commitment is to disseminate research and contributions of the International Scientific Community, academic institutions, agencies and entities of the public and private sectors and contribute to the linking of researchers who carry out scientific activities, technological developments and training of specialized human resources with governments, companies and social organizations.

Encourage the interlocution of the International Scientific Community with other Study Centers in Mexico and abroad and promote a wide incorporation of academics, specialists and researchers to the publication in Science Structures of Autonomous Universities - State Public Universities - Federal IES - Polytechnic Universities - Technological Universities - Federal Technological Institutes - Normal Schools - Decentralized Technological Institutes - Intercultural Universities - S & T Councils - CONAHCYT Research Centers.

Scope, Coverage and Audience

Journal Electrical Engineering is a Research Journal edited by ECORFAN-Mexico S.C in its Holding with repository in Republic of Peru, is a scientific publication arbitrated and indexed with semester periods. It supports a wide range of contents that are evaluated by academic peers by the Double-Blind method, around subjects related to the theory and practice of Electromagnetism, electrical distribution sources, electrical engineering innovation, signal amplification, electric motor design, material science in power plants, management and distribution of electrical energies with diverse approaches and perspectives , That contribute to the diffusion of the development of Science Technology and Innovation that allow the arguments related to the decision making and influence in the formulation of international policies in the Field of Engineering and Technology. The editorial horizon of ECORFAN-Mexico® extends beyond the academy and integrates other segments of research and analysis outside the scope, as long as they meet the requirements of rigorous argumentative and scientific, as well as addressing issues of general and current interest of the International Scientific Society.

Editorial Board

Arbitration Committee

Assignment of Rights

The sending of an Article to Journal Electrical Engineering emanates the commitment of the author not to submit it simultaneously to the consideration of other series publications for it must complement the Originality Format for its Article.

The authors sign the Authorization Format for their Article to be disseminated by means that ECORFAN-Mexico, S.C. In its Holding Republic of Peru considers pertinent for disclosure and diffusion of its Article its Rights of Work.

Declaration of Authorship

Indicate the Name of Author and Coauthors at most in the participation of the Article and indicate in extensive the Institutional Affiliation indicating the Department.

Identify the Name of Author and Coauthors at most with the CVU Scholarship Number-PNPC or SNI-CONAHCYT- Indicating the Researcher Level and their Google Scholar Profile to verify their Citation Level and H index.

Identify the Name of Author and Coauthors at most in the Science and Technology Profiles widely accepted by the International Scientific Community ORC ID - Researcher ID Thomson - arXiv Author ID - PubMed Author ID - Open ID respectively.

Indicate the contact for correspondence to the Author (Mail and Telephone) and indicate the Researcher who contributes as the first Author of the Article.

Plagiarism Detection

All Articles will be tested by plagiarism software PLAGSCAN if a plagiarism level is detected Positive will not be sent to arbitration and will be rescinded of the reception of the Article notifying the Authors responsible, claiming that academic plagiarism is criminalized in the Penal Code.

Arbitration Process

All Articles will be evaluated by academic peers by the Double-Blind method, the Arbitration Approval is a requirement for the Editorial Board to make a final decision that will be final in all cases. MARVID® is a derivative brand of ECORFAN® specialized in providing the expert evaluators all of them with Doctorate degree and distinction of International Researchers in the respective Councils of Science and Technology the counterpart of CONAHCYT for the chapters of America-Europe-Asia- Africa and Oceania. The identification of the authorship should only appear on a first removable page, in order to ensure that the Arbitration process is anonymous and covers the following stages: Identification of the Research Journal with its author occupation rate - Identification of Authors and Coauthors - Detection of plagiarism PLAGSCAN - Review of Formats of Authorization and Originality-Allocation to the Editorial Board- Allocation of the pair of Expert Arbitrators-Notification of Arbitration -Declaration of observations to the Author-Verification of Article Modified for Editing-Publication.

Instructions for Scientific, Technological and Innovation Publication

Knowledge Area

The works must be unpublished and refer to topics of Electromagnetism, electrical distribution sources, electrical engineering innovation, signal amplification, electric motor design, material science in power plants, management and distribution of electrical energies and other topics related to Engineering and Technology.

Presentation of the content

As the first article we present, *Development of an electronic stethoscope implementing filters with OPAM for the observation of cardiac signals using a graphical interface with an AD8232 module*, by GONZÁLEZ-GALINDO, Edgar Alfredo, RÍOS-MENDOZA, Fernando Javier, CASTRO-PÉREZ, Joseph Kevin and DOMÍNGUEZ-ROMERO, Francisco Javier, with affiliation at Universidad Nacional Autónoma de México, as the next article we present, *Comparative analysis of the conversion performance of a grid-connected photovoltaic system*, by BUENO-RIVERA, Raymundo, PORTILLO-JIMÉNEZ, Canek and BAJO-DE LA PAZ, Jorge Valentín, with adscription in the Universidad Autónoma de Sinaloa, as next article we present, *Energy and exergy analysis at the la joya sugar mill in Champotón, Campeche, Mexico*, by CHAN-GONZALEZ, Jorge J., CASTILLO-GAMBOA, Andrea, LEZAMA-ZÁRRAGA, Francisco and SHIH, Meng Yen, from the Universidad Autónoma de Campeche, as last article we present *Evaluation of the adherence of thermoplastic polyurethane (TPU) as an alternative material for the protection of solar cells*, by SALAZAR-PERALTA, Araceli, PICHARDO-SALAZAR, José Alfredo, PICHARDO-SALAZAR, Ulises and BERNAL-MARTÍNEZ, Lina, with affiliation at the TecNM: Tecnológico de Estudios Superiores de Jocotitlán, Centro de Bachillerato Tecnológico Industrial y de Servicios No. 161 and Centro de Estudios Tecnológicos Industrial y de Servicios No. 23.

Content

Article **Journal Electrical Engineering**
December 2023, Vol.7 No.19 1-14

Development of an electronic stethoscope implementing filters with OPAM for the observation of cardiac signals using a graphical interface with an AD8232 module

Desarrollo de un estetoscopio electrónico implementando filtros con OPAM para la observación de señales cardíacas utilizando una interfaz gráfica con un módulo AD8232

GONZÁLEZ-GALINDO, Edgar Alfredo†*, RÍOS-MENDOZA, Fernando Javier, CASTRO-PÉREZ, Joseph Kevin and DOMÍNGUEZ-ROMERO, Francisco Javier

Universidad Nacional Autónoma de México, Facultad de Estudios Superiore Aragón, Centro Tecnológic Aragón, Measurement and Instrumentation and Control Laboratory. Mexico.

ID 1st Author: *Edgar Alfredo, González-Galindo* / **ORC ID:** 0000-0003-4654-9595, **Researcher ID Thomson:** G-7927-2018, **CVU CONAHCYT ID:** 351785

ID 1st Co-author: *Fernando Javier Ríos-Mendoza* **/ ORC** ID 0009-0008-7125-0150, **Researcher ID Thomson:** HTS-9088-2023, **CVU CONAHCYT ID** 1039711

ID 2nd Co-author: *Joseph Kevin, Castro-Pérez* / ORC ID 0000-0001-6755-5260, **Researcher ID Thomson:** HJY-8903-2023, **CVU CONAHCYT ID** 1266037

ID 3rd Co-author: *Francisco Javier, Domínguez-Romero* / **ORC ID:** 0000-0003-0578-9322, **Researcher ID Thomson:** AFD-9764-2022, **CVU CONAHCYT ID:** 1037122

DOI: 10.35429/JEE.2023.19.7.1.14 Received July 10, 2023; Accepted December 30, 2023

Abstract

In this article, an investigation was developed in a clinic A low-cost electronic stethoscope has been developed, which utilizes fourth-order active filters and a TL081 operational amplifier preamplifier. It incorporates the AD8232 module for monitoring cardiac signals and features a graphical interface for visualizing these signals. A schematic circuit was designed for a second-order active filter with preamplifiers to compensate for signal attenuation, and electret microphones were used to replace the headphones. The device was implemented using an Arduino development board and a printed circuit board for connecting modules such as the AD8232, DS3231, and MicroSD. The system generates an audible signal through speakers, and the graphical interface facilitates the visualization of the electrical signal captured by the electrodes on the test subject. Data is recorded with date and time thanks to the DS3132 module and stored on the MicroSD module. The objective is to provide an affordable electronic stethoscope with a graphical interface that can be used in both medical clinics and homes during emergencies when access to a hospital electrocardiogram is not always possible. This low-cost solution provides an accessible and reliable tool for monitoring cardiac signals, improving healthcare in various clinical scenarios.

AD8232, DS3132, MicroSD

Resumen

Se ha desarrollado un estetoscopio electrónico de bajo costo que utiliza filtros activos de cuarto orden y un preamplificador con el amplificador operacional TL081. Incorpora el módulo AD8232 para monitoreo de señales cardíacas y cuenta con interfaz gráfica para visualizar dichas señales. Se diseñó un circuito esquemático para un filtro activo de segundo orden con preamplificadores para compensar la atenuación de la señal, y se reemplazaron los auriculares por micrófonos electret. El dispositivo se implementó con una tarjeta de desarrollo Arduino y un circuito impreso para conexión de módulos como AD8232, DS3231 y MicroSD. El sistema genera una señal audible a través de altavoces, y la interfaz gráfica facilita la visualización de la señal eléctrica capturada por los electrodos en el sujeto de prueba. Los datos se registran con fecha y hora gracias al módulo DS3132 y se almacenan en el módulo MicroSD. El objetivo es proporcionar un estetoscopio electrónico asequible con interfaz gráfica, válido tanto en consultorios médicos como en hogares durante emergencias, cuando no siempre es posible acceder a un electrocardiograma hospitalario. Esta solución de bajo costo brinda una herramienta accesible y confiable para el monitoreo de señales cardíacas, mejorando la atención médica en diversas situaciones clínicas.

AD8232, DS3132, MicroSD

Citation: GONZÁLEZ-GALINDO, Edgar Alfredo, RÍOS-MENDOZA, Fernando Javier, CASTRO-PÉREZ, Joseph Kevin and DOMÍNGUEZ-ROMERO, Francisco Javier. Development of an electronic stethoscope implementing filters with OPAM for the observation of cardiac signals using a graphical interface with an AD8232 module. Journal Electrical Engineering. 2023. 7-19:1-14.

* Correspondence to the author (E-mail: unam_alf@comunidad.unam.mx)
† Researcher contributing as first author.

Introduction

Today, cardiac problems can arise from two categories of causes. On the one hand, there are drugs, such as catecholamines, phosphodiesterase inhibitors, digitalis, beta-adrenergic stimulants and atropine. On the other hand, there are pathological processes, including cardiomyopathies, fibrosis, hyperkalaemia and ischaemia. In addition, it has been observed that severe acute respiratory syndrome, caused by SARS-CoV2, can have cardiac sequelae in the post-pandemic phase. This is because the severe cardiorespiratory distress caused by the virus can be further complicated if the individual has previous comorbidities. The World Health Organisation (WHO) provided data indicating that cardiovascular disease (CVD) is the leading cause of death worldwide.

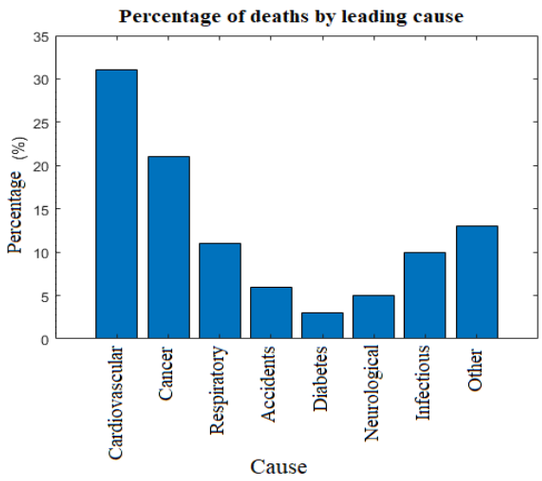

Graphic 1 Deaths from major diseases worldwide

In 2017, an estimated 17.9 million people died from CVD, accounting for 31% of all deaths worldwide. For the latest data, I would recommend searching for heart disease statistics on the WHO website or other reliable sources of public health information. When citing these sources, be sure to follow the correct citation format depending on the style you are using (WHO,2023). During 2021, heart disease emerged as the leading cause of death in Mexico, culminating in a total of 226,703 deaths. This number marked an increase of 8,000 deaths compared to the previous year. Among heart diseases, atrial fibrillation is the most prevalent arrhythmia worldwide, affecting approximately 40 million people. In Mexico, it is estimated that more than half a million people suffer from this condition (Bibiano, 2023).

The stethoscope was invented by French physician René Laennec in 1816. Laennec invented the stethoscope because he felt uncomfortable placing his ear on his patients' chests to listen to internal sounds, a common practice at the time (Roguin, 2006).

The stethoscope has gone through several modifications since René Laennec first invented it. However, one of the most notable changes was made by the Irish physician Arthur Leared in 1851. It was Leared who proposed the binaural design (two earpieces), which is the model that prevails to this day (Langfort, 1999). The stethoscope is a fundamental medical instrument used for auscultation, or listening to the internal sounds of the human body. In the 20th century, stethoscope technology continued to improve, with the introduction of electronic stethoscopes that could amplify body sounds for better diagnosis. Today, the stethoscope remains an essential tool in medical practice, used to listen to the sounds of the heart, lungs and abdomen (Bassetti, 2019). Therefore digital stethoscopes emerged as a superior option, offering sound amplification, more consistent frequency response and active noise cancellation. In addition, they have become a valuable tool for teaching auscultation due to their ease of recording and high sound quality. Some have taken advantage of these advances to create libraries of heart and lung sounds, providing an effective way to teach students this medical art (Arjoune, 2023).

It is noted that the characterisation of sounds through auscultatory signal recording, analysis and processing systems provides improved sensitivity and specificity in various studies. Furthermore, the availability of new representations of sounds, such as phonograms and spectrograms, not only opens up interesting perspectives in the context of diagnostic aids, but also in education and pedagogy (Emmanuel, 2016). This will allow medical students and trainees to perform realistic cardiac auscultations and listen to abnormal heart sounds in a clinical setting (Yhdego,2023).

ISSN: 2523-2517

The conversion of acoustic sound into an electrical signal requires a transducer. There are several types of transducers that can perform this function. The simplest method of sound detection is the use of a microphone in the chestpiece of the stethoscope. However, this technique has a drawback: it is susceptible to interference from ambient noise. An alternative is to place a piezoelectric crystal on the end of a metal shaft that is in contact with a diaphragm. Some manufacturers use more sophisticated methods, such as placing a piezo crystal inside a foam behind a diaphragm of considerable thickness, similar to rubber. Another technique involves the use of an electromagnetic diaphragm with a conductive inner surface that forms a capacitive sensor. This diaphragm responds to sound waves in a similar way to a conventional acoustic stethoscope, but with the difference that changes in the electric field replace changes in air pressure. The sound waves interacting with the condenser microphone generate a variation in its capacitance. This variation creates a voltage swing that is proportional to the amplitude of the incident sound waves. Correct positioning of the acoustic sensor relative to the microphone is essential to capture sound signals from the human body without noise interference. The microphone should be positioned as close as possible to the diaphragm. An electrical cable of sufficient length is provided linking the microphone to the connection plug, thus ensuring that there is room to properly position the sensor on the patient (Khandpur, 2020).

There are applications that describe in detail the setup of a system using the AD8232 module connected to an Arduino development board to acquire electrical signals from the heart. The AD8232 module is able to amplify and filter the ECG signal to obtain an accurate measurement, where a user interface is included in the form of a mobile application, which allows users to view and analyse the ECG data in real time, this application graphically displays the ECG waveform and provides information about the heart rate and possible cardiac abnormalities. This system shows a very good correlation between the data obtained between the application and traditional equipment found in hospitals and can be a viable alternative for cardiac monitoring (Prasad, 2019).

There are relevant developments such as the one carried out in Indonesia, where approximately 700,000 deaths per year are caused by heart attacks. To prevent heart attacks from becoming serious, early diagnosis is of utmost importance. One of the diagnostic techniques is the electrocardiogram (ECG). ECG devices record the electrical signal of the heart muscle to predict the presence of abnormalities in the heart. However, most of the existing ECG devices in Indonesia are found only in large hospitals. Patients with a heart attack have to wait for the ambulance to arrive and take them to the hospital. While waiting for the ambulance, the important signal associated with the heart attack may diminish, causing doctors to lose track of the causes of the heart attack. Other patients are too busy to have an ECG check unless something goes wrong with their heart. The ECG check is annoying. Therefore, it is very important to develop portable ECG devices. The portability of the devices will allow them to be placed in a Puskemas, which is a community health centre in Indonesia that offers primary health care services, and even in people's homes. Diagnosis will also be much easier and cheaper. Special conditions, such as heart attack patients, can also be taken care of with a portable ECG home care device (Gifari, 2015).

In this work a monitoring system was developed using a graphical interface developed with Matlab software, connected to an Arduino development board implementing an AD8232 module to visualise the behaviour of the acquired data and analyse ECG data, complemented with a stethoscope replacing the headphones with electret microphones connected to a preamplifier and fourth order active filters with Sallen-Key configuration, which could be beneficial for the diagnosis and monitoring of cardiac diseases, this proposed system seeks to provide an accessible and portable solution.

Aim

The main objective of this project is to design an electronic stethoscope using second order active filters and TL081CP operational amplifiers. The stethoscope will be intended to listen to the acoustic signals generated by the heart and lungs. In addition, a graphical interface will be designed using an Arduino UNO development board to acquire data.

ISSN: 2523-2517

For this, an AD8232 module will be used to compare the acoustic signal captured by the stethoscope with the signal coming from an ECG module. The collected data will be stored in a microSD memory by using a microSD card reader module. In addition, we plan to design a printed circuit board that will serve as the basis for assembling the Arduino UNO development board. This board design will facilitate the connection between the different modules used, such as the AD8232, RTC-DS3132 and the microSD card reader. The aim of this board is to avoid the excessive use of wires, reduce noise generation and minimise parasitic capacitances.

Hypothesis

In recent years, academics and students of the Electrical and Electronic Engineering course at the Facultad de Estudios Superiores Aragón at the Universidad Nacional Autónoma de México have faced challenges in the development of projects. One of the current challenges is to find innovative and creative solutions to address health issues in a society that has been seriously affected by the pandemic. In particular, the post-pandemic phase has left cardiac sequelae in patients who had comorbidities prior to SARS-CoV2. If an electronic stethoscope is developed that implements OPAM (Operational General Purpose Amplifier) filters for the observation of cardiac signals, using a graphical interface with an AD8232 module, then a significant benefit could be gained for the diagnosis and monitoring of cardiac disease, the system provides an accessible, portable and inexpensive solution to improve the detection and monitoring of cardiac disease.

Methodology and Development

This work was carried out in the Measurement, Instrumentation and Control Laboratory of the Centro Tecnológico Aragón of the FES. Aragón UNAM. A test board (Protoboard) was used to build a microphone preamplifier as shown in Figure 1, the eletcret will be adapted to the inside of the stethoscope ear tubes, an investigation on the use of low-pass filters to isolate low-frequency sounds was carried out.

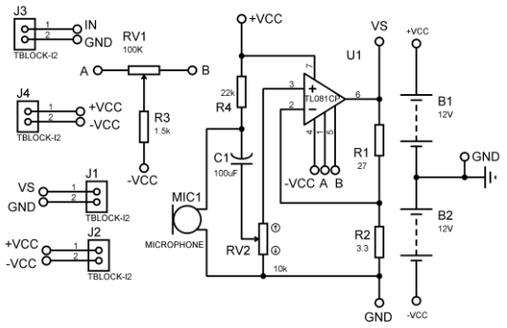

Figure 1 Circuit design for the cardiac signal preamplifier using an integrated TL081CP

Primarily, it is necessary to convert the heart sound into an electrical signal. To achieve this, a conventional stethoscope was modified by adding electro-acoustic (electret) microphones, as shown in Figure 1. In this way, the captured sound can be transformed into an electrical signal, which can then be processed by low-pass filters.

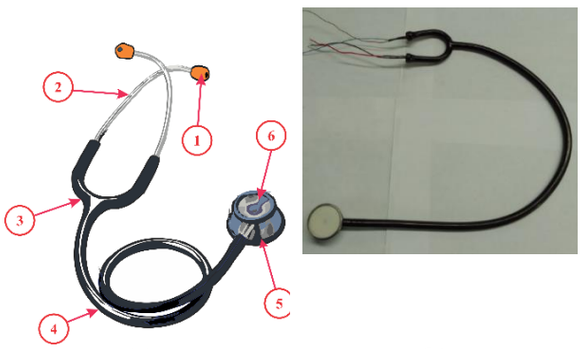

(a) (b)

Figure 2 a) Structure of the stethoscope. 1. Eyepieces 2. Earpieces 3. Bell. b) Modified stethoscope with two electret stethoscopes with preamplifier connection cables as shown in Figure 1.

The stethoscope, a fundamental instrument in medical practice, is used to amplify the internal sounds of the human body, facilitating auscultation. This device consists of several elements. Firstly, the end piece, which is placed on the patient's skin, has two parts: a semi-rigid membrane that is used to detect sounds of normal intensity, and a cup designed to capture softer sounds. When sound waves hit the membrane or bell, they begin to vibrate and amplify the sounds. The sound waves are then transmitted through a Y-shaped hose, made of a soft, flexible material, with a standard length of 40 cm.

ISSN: 2523-2517

The two ends of the "Y" are attached to two metal terminals (earpieces), each intended for one ear. These earpieces culminate in two ear-tips that fit snugly into the ear canal, capturing all transmitted sound and isolating outside noise that might interfere. In this way, the stethoscope allows the healthcare professional to clearly hear the internal sounds of the patient's body (Mesa, 2021). Recently, digital stethoscopes are replacing traditional stethoscopes due to their technological advantages in accuracy and data analysis. Auscultation, a widely used medical technique, becomes relevant with these advances, providing important details about cardiovascular and pulmonary diseases. Only medical experts in respiratory sounds, such as pulmonologists or cardiologists, can properly interpret these sounds and provide accurate diagnoses (Chitra, 2023).

Figure 3 shows a second-order low-pass filter circuit assembled on a test board. Although this system allows the heart sound to be heard through a loudspeaker, the intensity of the sound is low due to the attenuation of the acoustic signal as it passes through the filter. It should be noted that body noises are in the frequency range of 125 Hz to 3000 Hz, according to Lanuza (2019). However, due to the aforementioned attenuation, these sounds may not be easily perceptible.

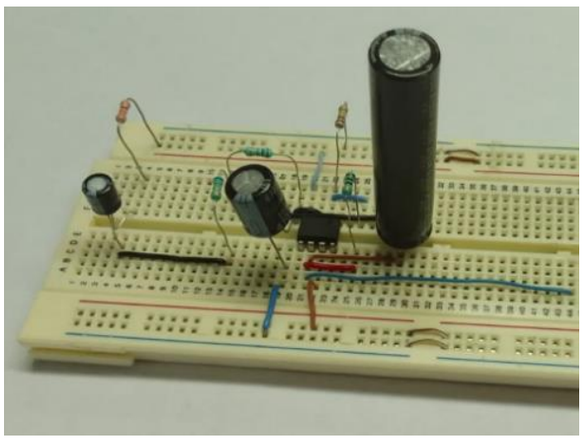

Figure 3 Breadboard circuit design of the preamplifier with a 10 gain op amp

The audio signal, once transformed into an electrical signal, is amplified by a preamplifier. Human heart sounds oscillate in a frequency range of about 20-200 Hz, while human lung sounds oscillate in a range of about 25-1500 Hz.

Most commercially available electronic stethoscopes offer several modes, including bell mode, diaphragm mode and extended range mode. These stethoscopes are equipped with a button or switch to change the frequency or mode, which may be located on the chestpiece, on a module integrated in the tube, or even directly on the main unit of the stethoscope. A set of filters is responsible for amplifying mid-range sounds, while attenuating sounds with extremely high or low frequencies. The extended range, on the other hand, is often referred to as wide, extended or organ mode.

A filter is a circuit or system designed to select, attenuate or eliminate certain frequency ranges within an input signal. It has both an input and an output. At the input, alternating signals with various frequencies are input, while at the output, these signals are extracted. Depending on the frequency of the signal, these can be attenuated to a greater or lesser extent. This filter, known as a low-pass filter, allows all frequencies from zero to a certain cut-off frequency to pass through, blocking all frequencies above this frequency. The frequencies between zero and the cutoff frequency are called the passband. On the other hand, frequencies above the cut-off frequency are called the passband or the attenuated band. The area between the passband and the removed band is known as the transition region (Mendoza, 2018).

Therefore, we have concluded that it is best to use a frequency of 690 Hz. This would allow us to effectively isolate the sound produced by the heart and lungs, allowing us to hear the acoustic waves more clearly. To achieve this goal, we sought to configure a second-order non-inverting Sallen-Key active low-pass filter.

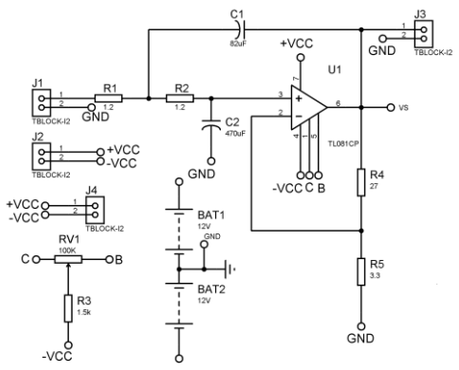

Figure 4 Schematic circuit design of a second-order Sallen-Key low-pass filter with a TL081CP housing

ISSN: 2523-2517

Figure 4 shows terminals B and C. Here, it can be seen that Pin 1 of the OPAM is connected to the first terminal of the component known as the trimmer (C), while Pin 5, according to the circuit diagram label, is connected to the third terminal of the trimmer (B).

In the data sheet for the ideal operational amplifier, the inverting input is denoted as V- or V_n, and is connected to terminal 2 of the package. On the other hand, the non-inverting input, which can be represented as V+ or V_p, is connected directly to terminal 3 of the TL081CP. This results in the voltages V_n and V_p at both terminals being equal, as shown in Equation 1 for an ideal operational amplifier. This condition is known as 'virtual balance', and is an important property of operational amplifiers, widely used in various circuits that require signal amplification or in filters that discriminate signals of certain frequencies. In certain experimental set-ups, small differences in input terminal voltages have been observed, attributable to component imperfections and external noise interference. However, for practical purposes, it was assumed that the voltages can be expressed as indicated in Figure 2 shows the B and C terminals. Here, it can be seen that Pin 1 of the OPAM is connected to the first terminal of the component known as the trimmer (C), while Pin 5, according to the circuit diagram label, is connected to the third terminal of the trimmer (B).

In the data sheet for the ideal operational amplifier, the inverting input is denoted as V- or V_n, and is connected to terminal 2 of the package. On the other hand, the non-inverting input, which can be represented as V+ or V_p, is connected directly to terminal 3 of the TL081CP. This results in the voltages V_n and V_p at both terminals being equal, as shown in Equation 1 for an ideal operational amplifier. This condition is known as 'virtual balance', and is an important property of operational amplifiers, widely used in various circuits that require signal amplification or in filters that discriminate signals of certain frequencies. In certain experimental set-ups, small differences in input terminal voltages have been observed, attributable to component imperfections and external noise interference. However, for practical purposes, it was assumed that the voltages can be expressed as follows.

$$V_n=V_p \tag{1}$$

In Figure 2 it can be seen that the input of pin 2 is connected to V_n with two connected resistors R_4 which would represent the feedback resistor R_f connected at the other end to V_s which indicates the output voltage of the filter represented with Pin 6 and R_5 is represented as R_i which together can be obtained as a voltage divider as shown in Equation 2.

$$V_n=\frac{R_i V_s}{R_i+R_f} \tag{2}$$

By subtracting the output voltage *Vs* from Equation 2.

$$V_s=\left(1+\frac{R_f}{R_i}\right)V_n \tag{3}$$

From Equation 3 we can substitute the part inside the parentheses and represent it as the closed-loop gain by Δv .

$$V_n=\frac{V_s}{\Delta v} \tag{4}$$

The equilibrium equations are established, starting at node V_x by applying Kirchhoff summation currents as shown in Equation 5.

$$\frac{V_p}{R_2}-\frac{V_x}{R_2}+V_p sC_2=0 \tag{5}$$

The second equilibrium equation is established at node V_x by applying Kirchhoff summation currents as shown in Equation 6,

$$\frac{V_x-V_i}{R_1}+\frac{V_x-V_p}{R_2}+\frac{V_x-V_s}{\frac{1}{sC_1}}=0 \tag{6}$$

From Equation 5 we obtain V_x

$$V_p(1+sR_2C_2)=V_x \tag{7}$$

From Equation 7 we apply the equality of Equation 1 and substitute Equation 4 to obtain the following equation as a function of V_s, where we will later have the ratio of the output voltage to the input voltage to visualise the transfer function of the second order low-pass filter.

$$\frac{V_s}{\Delta v}(1+sR_2C_2)=V_x \tag{8}$$

ISSN: 2523-2517

Starting from Equation 6 and developing the corresponding algebra, V_x is cleared and the following equation is obtained.

$$V_x=\frac{V_iR_2+V_pR_1+V_ssR_1R_2C_1}{R_2+R_1+sR_1R_2C_1} \quad (9)$$

From Equation 8 and Equation 9 both equations equal each other since they have the common term V_x, as follows.

$$\frac{V_s}{\Delta v}[1+sR_2C_2]=\frac{V_iR_2+\frac{V_s}{\Delta v}R_1+V_ssR_1R_2C_1}{R_2+R_1+sR_1R_2C_1} \quad (10)$$

Both sides of the equality we have the output voltage V_s, which is a common term and we have the input voltage V_i. Obtaining the ratio of the input voltage with respect to the output we have the following equation;

$$\frac{V_s}{V_i}=\frac{\Delta v}{s^2R_1R_2C_1C_2+s(R_1C_1+R_2C_2+R_1C_2-R_1C_1\Delta v)+1}$$

Simplifying the above equation:

$$\frac{V_s}{V_i}=\frac{\Delta v}{s^2R_1R_2C_1C_2+s\big(C_2(R_1+R_2)+R_1C_1(1-\Delta v)\big)+1} \quad (11)$$

This results in the transfer function as shown in Equation 12, where it can be seen in both the numerator and the denominator that the gain is involved in the polynomial.

$$H(s)=\left(\frac{\Delta v}{R_1R_2C_1C_2}\right)\left(\frac{1}{s^2+s\left(\frac{C_2(R_1+R_2)+R_1C_1(1-\Delta v)}{R_1R_2C_1C_2}\right)+\frac{1}{R_1R_2C_1C_2}}\right) \quad (12)$$

The angular cutoff frequency is given by ω_c

$$\omega_c^2=\frac{1}{R_1R_2C_1C_2}\rightarrow\omega_c=\sqrt{\frac{1}{R_1R_2C_1C_2}}\rightarrow\omega_c=\frac{1}{\sqrt{R_1R_2C_1C_2}} \quad (13)$$

The quality factor is given by

$$\frac{\omega_c}{Q}=\frac{C_2(R_1+R_2)+R_1C_1(1-\Delta v)}{R_1R_2C_1C_2}$$
$$Q=\frac{\omega_c(R_1R_2C_1C_2)}{C_2(R_1+R_2)+R_1C_1(1-\Delta v)}$$
$$Q=\frac{\frac{(R_1R_2C_1C_2)}{\sqrt{R_1R_2C_1C_2}}}{C_2(R_1+R_2)+R_1C_1(1-\Delta v)} \quad 14)$$

It can be seen that in Figure 2 the resistance R_1 and R_2 are equal $R_1=R_2=R$

$$H(s)=\left(\frac{\Delta v}{R^2C_1C_2}\right)\left(\frac{1}{s^2+s\left(\frac{(2C_2+C_1(1-\Delta v))}{RC_1C_2}\right)+\frac{1}{R^2C_1C_2}}\right) \quad (15)$$

Calculating the angular cutoff frequency which has as its units of $\left[\frac{rad}{s}\right]$

$$\omega_c=\frac{1}{R\sqrt{C_1C_2}} \quad (16)$$

If we condition that the values of the passive elements in this case the resistor $R_1=R_2$ and the capacitor $C_1=C_2$ are equal we have the following expression.

$$H(s)=\frac{\Delta v}{s^2R^2C^2+sRC(3-\Delta v)+1} \quad (17)$$

From the equation we normalise to identify the cut-off frequency as shown in the equation below:

$$H(s)=\left(\frac{\Delta v}{R^2C^2}\right)\left(\frac{1}{s^2+s\left(\frac{3-\Delta v}{RC}\right)+\frac{1}{R^2C^2}}\right) \quad (18)$$

Another way to represent the normalised transfer function is to replace the gain Δv with the variables of the resistors involved as follows R_f and R_i

$$H(s)=\left(\frac{1+\frac{R_f}{R_i}}{R^2C^2}\right)\left(\frac{1}{s^2+s\left(\frac{3-\left(1+\frac{R_f}{R_i}\right)}{RC}\right)+\frac{1}{R^2C^2}}\right) \quad (19)$$

Substituting the values of the resistances for the conductance gives the transfer function, which would be represented as shown in the following equation:

$$H(s)=\frac{\Delta vG_1G_2}{s^2C_1C_2+s(C_2(G_1+G_2)+C_1G_2(1-\Delta v))+G_1G_2} \quad (20)$$

By substituting the inverses of the resistors, when the balance equations are established at the time of the Kirchhoff current summation analysis, Equation 10 of the same transfer function can be arrived at. Gain as a function of voltage or power can be used.

$$dB=20\log_{10}(\Delta v)=20\log_{10}(1+\frac{R_f}{R_i}) \quad (21)$$

It should be noted that the dB voltage gain is only equal to the dB power gain if the input and output impedances of the system match.

ISSN: 2523-2517

$$dB_{rms}=20\log_{10}\left(\frac{\Delta v}{\sqrt{2}}\right)=20\log_{10}\left(\frac{1+\frac{R_f}{R_i}}{\sqrt{2}}\right) \quad (22)$$

To obtain the quality factor, it can be obtained as shown in the following equation.

$$Q=\frac{\sqrt{C_1C_2}}{\left(2C_2+C_1(1-\Delta v)\right)} \quad (23)$$

To make the Bode plot in magnitude and phase, the simplified Equation 12 was taken, taking the following values for its design, where: $R=R_1=R_2=1.2\Omega$, $C_1=82uF$, $C_2=470uF$, $R_f=27\Omega$ and $R_i=3.3\Omega$ the frequency used is f =675 Hz the calculation of the angular frequency is $\omega_c=4244.9\left[\frac{rad}{s}\right]$ this comes from Equation 13, to calculate the Gain $\Delta v=1+\frac{R_f}{R_i}=9.1818$ the unit of this is dimensionless, if we take this value we can obtain the decibels applying Equation 18 giving as a result dB=19.2586 and to obtain the decibels of the root mean square is obtained from Equation 19 and gives as a result $dB_{rms}=16.2483$ which is exactly where it cuts the angular cutoff frequency, its quality factor Q= 0.7296 is also obtained through Equation 20. Therefore, substituting the values of the passive elements in the transfer function would be as shown in Equation 19.

$$H(s)=\left(\frac{9.182}{5.55\times10^{-8}\,s^2+0.0003229\,s+1}\right) \quad (24)$$

Graph 2, which is derived from Equation 19, represents the Bode plot in phase and magnitude. It can be seen that its behaviour is consistent with a second-order low-pass filter, since a decade later it drops by 40dB. In the magnitude diagram, the blue arrow indicates exactly where the angular frequency intersects the root-mean-square decibels (〖dB〗 _rms). In the phase diagram, also indicated by a blue arrow, it can be seen that the cut-off angular frequency intersects at 90°.

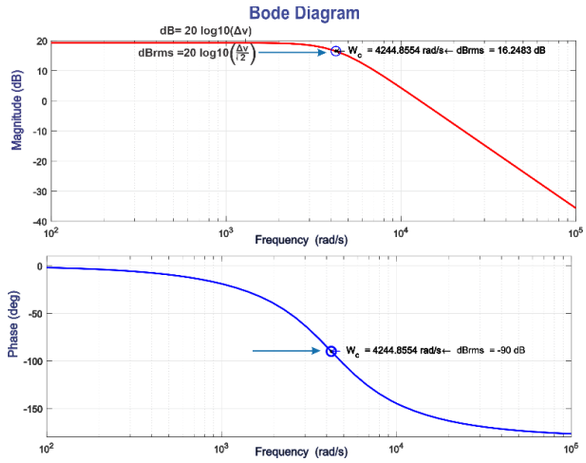

Graphic 2 Bode plot in magnitude and phase showing the cutoff angular frequency

In Graph 3, it shows the bode diagram in magnitude and phase, using the simulation program called proteus, the proposed schematic circuit was designed to implement it in the electronic stethoscope in order to filter the noise signals, noting that both graphs coincide showing the same value of ω_c and dB_{rms}.

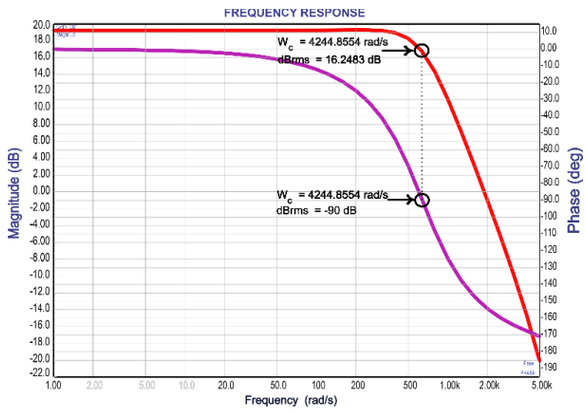

Graphic 3 Simulation using proteus of the Bode plot in magnitude and phase

For the volume control in the speaker connected to the stethoscope, a preamplifier was designed, which uses a TL081CP operational amplifier as shown in the 3D design of figure 5.

ISSN: 2523-2517

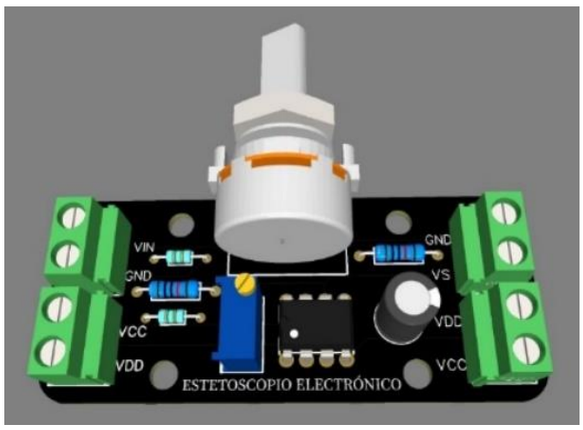

Figure 5 3D printed circuit of the preamplifier with a TL081CP package.

Figure 6 presents the three-dimensional layout of the printed circuit for the Sallen-Key second-order active low-pass filter. This circuit is composed of passive elements that will be connected to the preamplifier. In turn, these elements will receive power from the power supply of the same preamplifier. At the output of the circuit, a connection to the loudspeaker will be made.

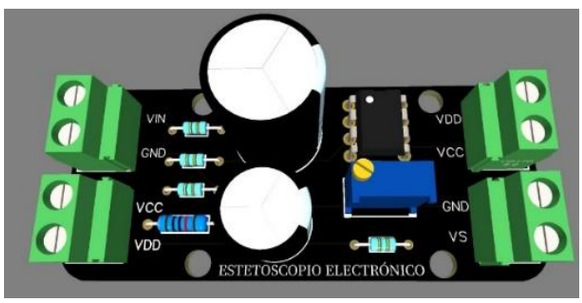

Figure 6 Three-dimensional printed circuit board of a non-inverting active second-order low-pass filter

Figure 7 shows the layout of the printed circuit in which the passive components, such as the resistor and the capacitor, will be mounted. The terminal blocks will also be installed, which will allow energy to be transferred from one plate to another, and transmit the acoustic signal from the stethoscope so that it can be heard through the loudspeaker.

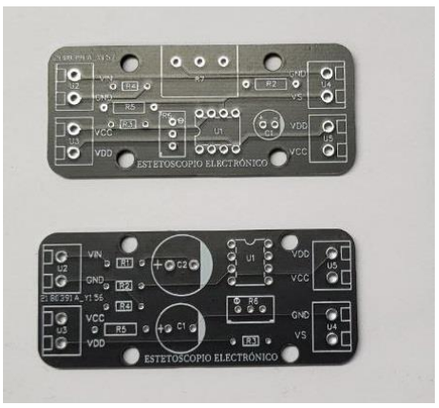

Figure 7 Active 2nd Order Low Pass Filter and Preamplifier PCB

It is crucial to properly layout the printed circuit board with the corresponding traces, which will allow the manufacturer to silk-screen print the precise dimensions. This layout is essential during component assembly, as it facilitates the identification of polarisation indications and the correct placement of integrated circuits. By following these guidelines, the generation of short circuits can be prevented, as illustrated in Figure 8.

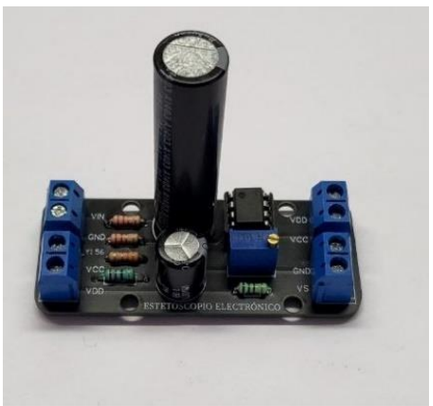

Figure 8 Electronic circuit board with the passive elements of the second order active low-pass filter to be assembled to the preamplifier and the speaker

For the design of the graphical interface of the electronic stethoscope, a printed circuit board was developed that allows the integration of the Arduino UNO development board with various modules. These modules include the AD8232, the RTC-DS3132 and a MicroSD Reader. These components are assembled and connected according to the schematic circuit shown in Figure 3.

ISSN: 2523-2517

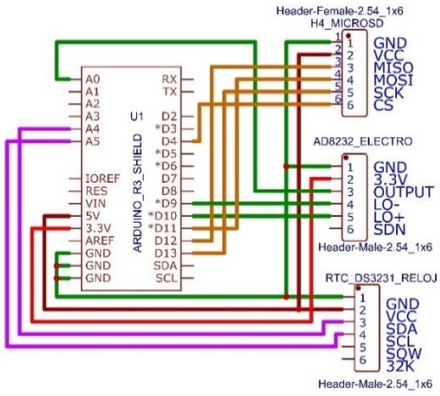

Figure 9 Design of the shelft schematic circuit to attach it to the Arduino development board and mount the modules RTC-DS3231, AD8232 and the MicroSD module

Figure 7 presents the design of a three-dimensional printed circuit board, developed using online computer-aided design software. This design clearly details the silk-screen printing of the modules to be used for the experiment.

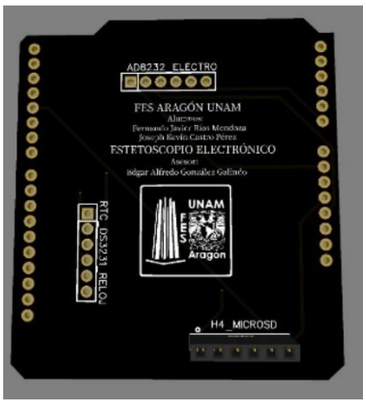

Figure 10 3D printed circuit board for connection between Arduino uno and AD8232 modules, RTC-DS3132, microSD card reader

The physical design of a printed circuit board (PCB) is of great importance due to the many advantages it offers during operation. One of the main advantages is the elimination of much of the noise that is often generated by the connection cables, which can act as electrical dipoles. The purpose of this design is to facilitate the assembly and disassembly of each module. For this reason, female connectors have been incorporated into the design to allow easy replacement by the operator in the event of damage. This can be seen in Figure 8.

Figure 11 Printed circuit board for connection of AD8232, RTC-DS3132, microSD card reader modules

Image 8 below shows the development board used in the experimental setup, as well as the printed circuit board that will be placed on top of the Arduino UNO.

Figure 12 Printed circuit board for the connection between the Arduino uno and the modules AD8232, RTC-DS3132, microSD card reader

The modules used that will be mounted on the PCB layout are shown in Figure 10, together with the development board and the PCB circuit.

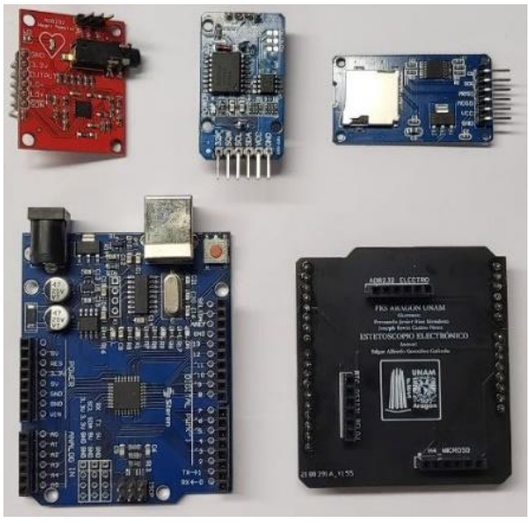

Figure 13 AD8232, RTC-DS3132 and microSD card reader modules, together with development board and PCB

ISSN: 2523-2517

Figure 11 shows the assembly of the AD8232, RTC-DS3132 and microSD card reader modules on the PCB mounted on the Arduino UNO.

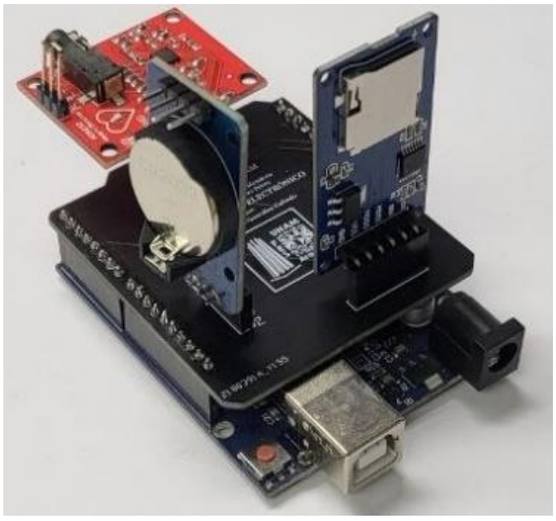

Figure 14 Printed circuit board with the assembled modules on the Arduino UNO development board

The following code is used to obtain data from the ECG module. This code collects information such as date, time and data logging for the electrical signal. The collected sampling is used to plot the electrical signal using the serial plotter in the Arduino integrated development environment (IDE).

```
//Se incluyen las siguientes librerías para poder programar los módulos
#include <Wire.h>
#include <RTClib.h>
#include <SD.h>
#include <SPI.h>
//Inicializar el objeto para manejar la lectura del RTC-DS3132
RTC_DS3231 rtc;
//Variable para guardar el tiempo actual del RTC
DateTime now;
//Variable para guardar la lectura del AD8232
int ecgValue;
//Variable para el nombre del archivo en la tarjeta microSD
char filename[] = "dataecg.txt";
//Variable para el pin CS del módulo lector de microSD
const int chipSelect = 4;
void setup() {
  //Inicializar el puerto serie
  Serial.begin(9600);
    //Inicializar la comunicación con el RTC
  Wire.begin();
  rtc.begin();
    //Inicializar la comunicación con la tarjeta microSD
  if (!SD.begin(chipSelect)) {
    Serial.println("Error al inicializar la tarjeta microSD.");
    return;
  }
    //Crear el archivo para guardar las lecturas
  File dataFile = SD.open(filename, FILE_WRITE);
    //Verificar si se pudo crear el archivo
  if (dataFile) {
    dataFile.println("Fecha, Tiempo, ampm, Valor ECG");
    dataFile.close();
    Serial.println("Archivo creado.");
  } else {
    Serial.println("Error al crear el archivo.");
  }
}
void loop() {
  //Leer el tiempo actual del RTC
  now = rtc.now();
    //Leer el valor del AD8232
  ecgValue = analogRead(A0);
    //Abrir el archivo para agregar una nueva lectura
  File dataFile = SD.open(filename, FILE_WRITE);
    //Verificar si se pudo abrir el archivo
  if (dataFile) {
    //Agregar la lectura al archivo
    dataFile.print(now.year(), DEC);
    dataFile.print('/');
    dataFile.print(now.month(), DEC);
    dataFile.print('/');
    dataFile.print(now.day(), DEC);
    dataFile.print(',');
    dataFile.print(' ');
    dataFile.print(now.hour(), DEC);
    dataFile.print(':');
    dataFile.print(now.minute(), DEC);
    dataFile.print(':');
    dataFile.print(now.second(), DEC);
    dataFile.print(',');
    dataFile.println(ecgValue);
    dataFile.close();
    //Imprimir la lectura en el puerto serie
    Serial.print(now.year(), DEC);
    Serial.print('/');
    Serial.print(now.month(), DEC);
    Serial.print('/');
    Serial.print(now.day(), DEC);
    Serial.print(',');
    Serial.print(' ');
    Serial.print(now.hour(), DEC);
    Serial.print(':');
    Serial.print(now.minute(), DEC);
    Serial.print(':');
    Serial.print(now.second(), DEC);
    Serial.print(',');
    Serial.println(ecgValue);
  } else {
    Serial.println("Error al abrir el archivo.");
  }
    //Esperar un segundo antes de tomar otra lectura
  delay(1000);
}
```

Results

Figure 11 shows the configuration of eight modules each comprising the preamplifiers and the second order active low-pass filters. These modules are combined to form a fourth order filter.

ISSN: 2523-2517

The output signals from these modules are connected to an audio amplifier, which in turn is connected to the loudspeakers. Both the loudspeakers and the complete system are powered by a voltage source for proper biasing. To carry out the tests, a high-performance subject was selected. Over a period of 30 minutes, acoustic sounds corresponding to the subject's heart rate were recorded and obtained.

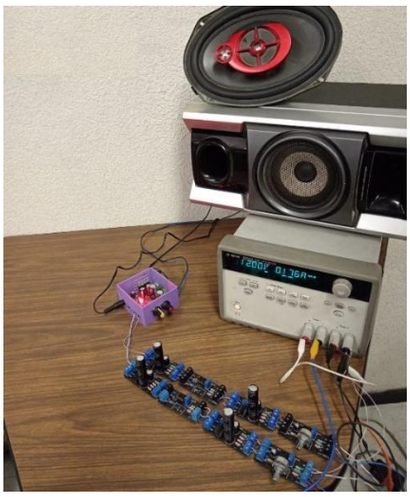

Figure 15 Experimental arrangement integrated by modules of the filters using and of the audio amplifier

During the test to obtain the acoustic signal of the heart rate, the subject was asked to maintain a proper position, as shown in Figure 12, and was instructed to remove the T-shirt to allow for proper auscultation. The subject was instructed to maintain normal breathing and muscle relaxation to facilitate an accurate assessment. As a result, a clear heart rate signal was obtained, ruling out other acoustic signals coming from the same subject, such as abdominal sounds, vascular sounds and joint sounds. This allowed a better focus on the auscultation of the heart rhythm and contributed to a more accurate assessment.

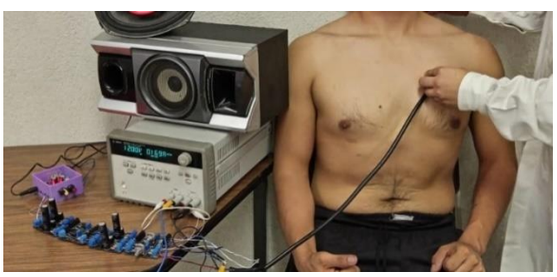

Figure 15 Test carried out on a subject, after physical activity, using a Sallen-Key fourth-order active low-pass filter

The results of connecting the modules to observe the synchronisation between the acoustic signal and the behaviour of the electrical signal coming from the AD8232 module are presented below, as illustrated in Figure 13. During the tests, it was possible to simultaneously obtain a visual representation of the electrical signal and the perception of an acoustic signal corresponding to the heart rhythm. This approach allowed the visualisation and auditing of the electrical and acoustic activity of the heart together, providing a comprehensive and complementary assessment of the heart rhythm during the test period.

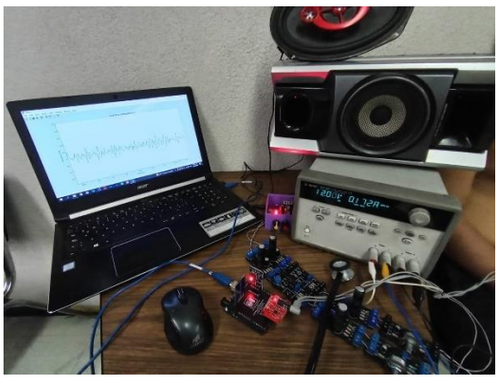

Figure 16 Experimental fix implementing the modules AD8232, RTC-DS3132, microSD card reader. Visualizing in a graphical interface the electrical signal coming from the heart rate.

A visual representation of the data recorded by the AD8232 module was obtained in Graph 4, where the amplitude variations that are characteristic of a cardiac signal can be clearly observed.

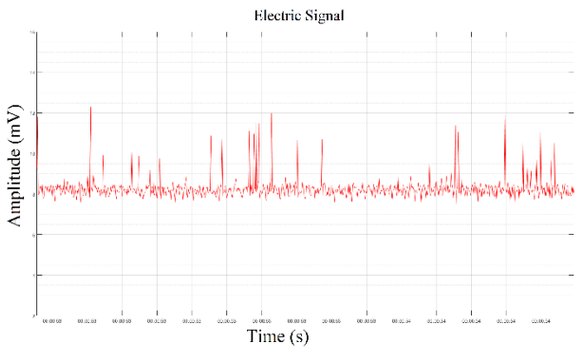

Graphic 4 Record of the electrical signal displayed in real time through the graphical interface from the AD8232 module

ISSN: 2523-2517

The initial electrical signal, captured by the AD8232, was subjected to processing using a digital band-pass filter. This filter was designed to eliminate certain signals with specific frequencies, which allowed a smoother signal to be obtained, free of unwanted interference. The results of this processing are presented in Figure 5.

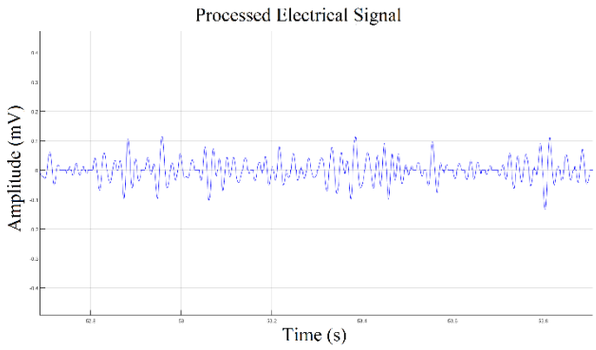

Graphic 5 Electrical signal passed through the digital fifth order band-pass filter

Conclusion

An electronic stethoscope has been designed and developed using second order active filters with TL081CP operational amplifiers. This will allow the acoustic signals generated by the heart and lungs to be heard clearly and accurately in a loudspeaker and by using a graphic interface implemented on an Arduino UNO development board, it has been possible to acquire and visualise the data collected by the ECG module. This interface will provide students of Electrical and Electronic Engineering and Medicine with a practical and user-friendly tool for monitoring cardiac and respiratory signals. The integration of the AD8232 module has made it possible to compare the acoustic signal captured by the stethoscope with the signal coming from an ECG module. This comparison provides greater accuracy in the diagnosis and analysis of cardiac signals. Data collected during measurements are conveniently stored on a microSD memory, using an SD card reader module. This ensures data availability and portability for further analysis and review. The design of a printed circuit board specifically for this project has enabled an efficient connection between the different modules used, reducing noise generation and minimising parasitic capacitances compared to using a test board called Protoboard.

This improves the quality of the acquired electrical signals and provides a stable platform for the operation of the electronic stethoscope. In summary, the stated objectives have been met by developing a functional electronic stethoscope with cardiac and respiratory signal acquisition and display capabilities. This device presents advantages in terms of cost, accuracy, portability and ease of use, which contributes to improving medical care in diverse clinical situations. The work presented in this article will allow, in the future, the characterisation of electrical signals used in robotic prostheses.

Acknowledgements.

The authors would like to thank the Coordination of the Technological Centre of the Facultad de Estudios Superiores Aragón and the Electrical and Electronic Engineering Department of the Universidad Nacional Autónoma de México, for the facilities provided through agreements with different software companies. We would also like to thank Jorge Ríos Mendoza for his technical support to this project.

References

Organización Mundial de la Salud. (2023). Enfermedades cardiovasculares. Recuperado de https://www.who.int/es/news-room/fact-sheets/detail/cardiovascular-diseases-(cvds)

Bibiano Mejía, I., & González Galindo, E. A. (2023). Diseño e implementación de una tarjeta de circuito impreso para acoplar módulos y generar un instrumento electrónico de medición de pulso y oxígeno para detección de cardiopatías y control de medicamentos en pacientes diagnosticados. http://132.248.9.195/ptd2023/abril/0838030/Index.html

Roguin, A. (2006). Rene Theophile Hyacinthe Laënnec (1781–1826): The Man Behind the Stethoscope. Clinical Medicine & Research, 4(3), 230–235. https://doi.org/10.3121/cmr.4.3.230

Langfort J, Ploug T, Ihlemann J, Saldo M, Holm C, Galbo H. Expression of hormone-sensitive lipase and its regulation by adrenaline in skeletal muscle. Biochem J. 1999 Jun 1;340 (Pt 2)(Pt 2):459-65. PMID: 10333490; PMCID: PMC1220272.

ISSN: 2523-2517

Emmanuel Andrès, Raymond Gass (2016), Stethoscope: A Still-Relevant, Tool and Medical Companion, The American Journal of Medicine,Volume 129, Issue 5, 2016, Pages e37-e38. https://doi.org/10.1016/j.amjmed.2015.06.046.

Yhdego, H., Kidane, N., Mckenzie, F. y Audette, M. (2023). Desarrollo de modelos de aprendizaje profundo para una simulación híbrida de entrenamiento de auscultación en pacientes estándar utilizando un estetoscopio de patología virtual basado en ECG. SIMULACIÓN , 00375497231165049. https://doi.org/10.1177/00375497231165049

A. S. Prasad and N. Kavanashree, "ECG Monitoring System Using AD8232 Sensor," 2019 International Conference on Communication and Electronics Systems (ICCES), Coimbatore, India, 2019, pp. 976-980, https://doi:10.1109/ICCES45898.2019.9002540.

M. W. Gifari, H. Zakaria and R. Mengko, "Design of ECG Homecare:12-lead ECG acquisition using single channel ECG device developed on AD8232 analog front end," 2015 International Conference on Electrical Engineering and Informatics (ICEEI), Denpasar, Indonesia, 2015, pp. 371-376, https://doi:10.1109/ICEEI.2015.7352529.

Mesa, A. L. U., & Moreno, D. U. (2021). Manual para el examen físico del normal y métodos de exploración. Corporación para investigaciones Biológicas CIB. URL: https://books.google.com.mx/books?id=mtQwEAAAQBAJ&pg=SA4-PA25&dq=estetoscopio+electr%C3%B3nico&hl=es-419&sa=X&ved=2ahUKEwiywsD1vsL8AhVgEUQIHXsmA04Q6AF6BAgJEAI#v=onepage&q=estetoscopio%20electr%C3%B3nico&f=false

R. Chitra, N. Jayapreetha, D. Swetha y S. Swetha, "Digital Stethoscope For Instant Monitoring For Cardiac Auscultation", Conferencia internacional de 2023 sobre señales biológicas, imágenes e instrumentación (ICBSII) , Chennai, India, 2023, págs. 1-6, https://doi:10.1109/ICBSII58188.2023.10181065

Lanuza Centeno, J. E., & Moncada Flores, C. A. (2019). Variación de los niveles de presión arterial en los pacientes sometidos a procedimientos de exodoncia en las clínicas de cirugía oral y diagnóstico de la Facultad de Odontología de la UNAN -León, en el período de agosto a noviembre del año 2017 y octubre a diciembre del año 2018, URL: http://riul.unanleon.edu.ni:8080/jspui/bitstream/123456789/7687/1/244159.pdf

Khandpur, R. S. (2020). *Compendium of biomedical instrumentation*. John Wiley & Sons, Incorporated. URL:https://www.proquest.com/docview/2319746494?accountid=14598&parentSessionId=nGD4xNVuUP3RGwMU1T4%2BcQSSOCs26ePQc9z4iL%2B4f0E%3D

Mendoza Corona, J. A., & Pérez López, M. A., (2018), Filtro pasa bajas con capacitores conmutados. URL: https://tesis.ipn.mx/bitstream/handle/123456789/27828/TESIS-FINAL.pdf?sequence=1&isAllowed=y

ISSN: 2523-2517

Article **Journal Electrical Engineering**
December 2023, Vol.8 No.19 15-24

Comparative analysis of the conversion performance of a grid-connected photovoltaic system

Análisis comparativo del rendimiento de conversión de un sistema fotovoltaico conectado a la red

BUENO-RIVERA, Raymundo†, PORTILLO-JIMÉNEZ, Canek* and BAJO-DE LA PAZ, Jorge Valentín

Universidad Autónoma de Sinaloa, Facultad de Ingeniería, Av. De las Américas y Blvr. Universitarios, S/N, Ciudad Universitaria, C.P. 80013, Culiacán, Sinaloa, México.

ID 1st Author: *Raymundo, Bueno-Rivera* / **ORC ID:** 0009-0001-7742-267X

ID 1st Co-author: *Canek, Portillo-Jiménez* / **ORC ID:** 0000-002-3063-3699, **CVU CONAHCYT ID:** 42353

ID 2nd Co-author: *Jorge Valentín, Bajo-De la Paz* / **ORC ID:** 0009-0009-1421-4708

DOI: 10.35429/JEE.2023.19.7.15.24 Received July 15, 2023; Accepted December 30, 2023

Abstract

A performance study of a photovoltaic system installed in an eco-house on the campus of the University of Calgary in Canada is presented. The panels of the photovoltaic array installed on the roof have different azimuth and tilt angles, therefore, the solar energy incident on them is different. The effects of orientation on the efficiency of electrical energy production in individual photovoltaic modules are analyzed. The conversion efficiency is determined by means of measurements of the energy produced by the modules, supported by the RETScreen software, but also independently, it is calculated using the radiation data from the university weather station (WRS). These results are compared with those of a previous study, carried out with PVSyst, where the orientation angles of the system are simplified. Average results of energy produced, and efficiency are shown. It is observed that the efficiencies from the simulations are very similar, although of lower value. The results obtained with WRS are considered more realistic and of greater magnitude.

Solar energy production, Solar radiation measurements, Simulation efficiencies comparison

Resumen

Se presenta un estudio de rendimiento de un sistema fotovoltaico instalado en una casa ecológica en el campus de la Universidad de Calgary en Canadá. Los paneles del arreglo fotovoltaico instalados en el techo, tienen diferentes ángulos de acimut e inclinación. Se analizan los efectos de la orientación en la eficiencia de producción de energía eléctrica en los módulos fotovoltaicos individualmente. Se determina la eficiencia de conversión por medio de mediciones de energía producida por los módulos, apoyándose con el software RETScreen, pero también de forma independiente, se calcula utilizando los datos de radiación de la estación meteorológica de la universidad (WRS). Estos resultados, se comparan con los de un estudio previo realizado con PVSyst, donde se simplifica los ángulos de orientación del sistema. Se muestran resultados promedio de energía producida, y de eficiencia. Se observa que las eficiencias a partir de las simulaciones son muy parecidas, aunque de menor valor. Los resultados obtenidos con WRS se consideran más realistas y de mayor magnitud.

Comparación de simulación de eficiencias, Mediciones de radiación solar, Producción de energía solar

Citation: BUENO-RIVERA, Raymundo, PORTILLO-JIMÉNEZ, Canek and BAJO-DE LA PAZ, Jorge Valentín. Comparative analysis of the conversion performance of a grid-connected photovoltaic system. Journal Electrical Engineering. 2023. 7-19:15-24.

* Correspondence to Author (E-mail: canekportillo@uas.edu.mx)
† Researcher contributing as first author.

Introduction

There are several research studies where the importance of studying the efficiency of photovoltaic systems (PVS) is shown, proposing techniques, algorithms, or models to maximize it. For example, one of the techniques that allows increasing performance in a PVS is the maximum power point tracking (MPPT). Various proposals have been made, experimenting with the combination of already existing algorithms for the control of the MPPT, demonstrating its effectiveness in simulation-based implementations (Manas M. et al., 2023).

Furthermore, in other works the authors validate their proposals in hardware, applying techniques and addressing topics related to artificial intelligence, such as neural networks and machine learning (Jena R. et al. 2023). In (Song Y. et al, 2023), a mixed power generation system, where the inclusion of a PVS is a substantial part, is proposed. In addition, the authors establish a model that optimizes or allows the most appropriate conditions for better efficiency in energy production. On the other hand, in (N. Kahar N. et al., 2023) the authors carried out a comparative study, where they demonstrate through simulation, that the use of PV systems with bifacial panels increases the efficiency in PVS.

Nevertheless, initially the investment cost could be significant. In (Galicia R, et al., 2023) the authors implement a study of a photovoltaic (PV) panel to observe how the specific environmental conditions of a geographical point affect it. The author mention that the influence of temperature, solar radiation, humidity, and wind speed on the efficiency of the solar panel was the main research motivation. In the current paper, a performance study of a photovoltaic system installed in an eco-house on the campus of the University of Calgary in Canada is presented. There is a roof made up of 37 PV panels, where two of them are horizontal, while the rest are oriented according to a certain curvature of the roof design, resembling a tortoise shell. Moreover, there are seven rows of five modules connected in a parallel configuration, each with an individual inverter (microinverter) that can record the electricity production of each PV module in real time.

This research focuses on the determination of the performance of this PV system, analyzing the figure of merit of conversion efficiency (the division of electrical energy produced at the output of the module between the energy that affects the module through solar radiation). There is already an analysis of this system based on simulation (Team Canada, 2011) where the PVSyst software is used, and it is validated with SAM-NREL. Although both previous results are very approximate, certain considerations were made in the study due to limitations in the database device data (PV modules). The authors are even aware that, owing to the design, there is a variation in the orientation of the panels in terms of azimuth, which according to their calculations is 9.5° on average, but for simulation purposes they establish 9° in average for the entire PV generator. In the present work, the performance is reviewed if more realistic conditions are considered.

In fact, each row of modules presents different orientations and therefore variations in azimuth. For this reason, in (Bueno R, 2015), information about the PV system has been collected, as part of the work developed in an international summer stay at the University of Calgary. The information collected consists of the physical characteristics of the PV system and the energy production data, which allow obtaining the efficiency of each module. In addition, the free software RETScreen is considered, which provides data such as irradiance, which is required to calculate the energy produced by the modules per day, as well as the efficiency. The above is validated; that is, the calculation is carried out again, but now with meteorological information obtained directly from the university's meteorological station (WRS).

On the one hand, this information is taken up and a comparative analysis is accomplished between the efficiency results obtained from the use of RETScreen and that obtained from the WRS information’s. On the other hand, these results are compared with the information from the previous analysis, where the PVSyst is used (Team Canada, 2011). It is considered that this study allows to have a more realistic performance behavior of the PV array than in the previous study, by considering the real azimuth angles instead of a single average value.

ISSN-2523-2517

Moreover, it is considered that, by determining the efficiency from data taken directly from the meteorological station located very close to the study system, it allows obtaining information with greater accuracy. The rest of the article is made up of the following sections: section 2 presents the physical and electrical characteristics of the photovoltaic system; the methods used to assess conversion performance are explained in section 3; the results and discussion are in section 4; finally, in section 5 the conclusions are shown.

Study PV system

Physical characteristics

Figure 1 shows the installation of the arrangement of 35 PV modules on the roof of the house, forming a somewhat elliptical silhouette. Seven groups of five PV modules with the same geometric characteristics are formed. The panels of the different sections have a very similar inclination, but their azimuth angle does vary significantly, especially for the modules installed in sections that are further apart. Therefore, to carry out an analysis of the performance in energy production, it is necessary to consider seven flat surfaces with different geometric characteristics, since, due to the difference in angles, the irradiance incident on them will also vary. Section one is called the section that is furthest to the West and section seven is the one that is furthest to the East (as shown in Table 1).

Figure 1 Spo'pi house on the campus of the University of Calgary
Source: Own elaboration

Direction	West ----------> East						
Section	1	2	3	4	5	6	7

Table 1 Distribution of PV array sections
Source: Own elaboration

Therefore, it is necessary to know the azimuth angle and the inclination that each of the sections has. The design of the house was made by computer, and it has a 3D drawing. From this, the desired angles can be determined, since all the measures defined in the design were respected, both for accommodation in the direction of the house towards the south and in the structure that supports the arrangement.

Determination of the azimuth angle with the CAD model

To determine the angles, we work with the Revit model of the project (see figure 2).

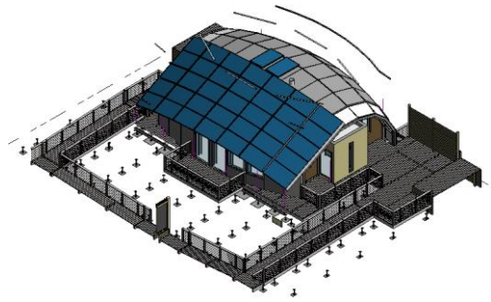

Figure 2 Revit model of the Spo'pi house, Canada Solar Decathlon

To carry out the calculations and the desired measurements, this model has been exported to AutoCAD. When making this format change, the Revit model works with many lines for details. Figure 3 shows the already exported drawing again.

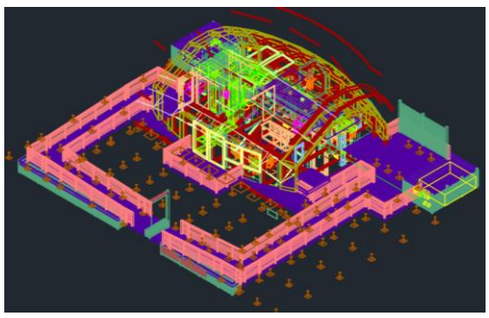

Figure 3 Autocad model of the Spo'pi house, Canada Solar Decathlon

Of the elements included in the drawing, only those corresponding to the installation of the photovoltaic modules are of interest.

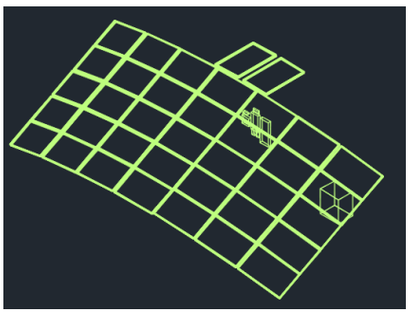

Figure 4 Drawing in autocad for the calculation of azimuth
Source: Own elaboration

For this reason, we proceed to hide all the other layers of the drawing, until only the block of lines that forms the photovoltaic array is shown (figure 4). Autocad has a method to measure the azimuth angle of a line, it calculates it with respect to the normal of the line and its projection towards the south, in the drawing records. When doing the export, the data of the geographic position with respect to the south are also sent. Therefore, parallel lines are drawn to each one of the sections to be able to use this method, until obtaining a drawing like the one shown in figure 5. As can be seen, there are already parallel lines to the different sections of the array, so the method can be applied. This consists of selecting one of the lines, right clicking with the mouse on it and writing the Field command. This command opens a dialog box in which object is subsequently chosen in field names and angle in property. With this selection the calculation of the azimuth angle is made showing it in the preview box.

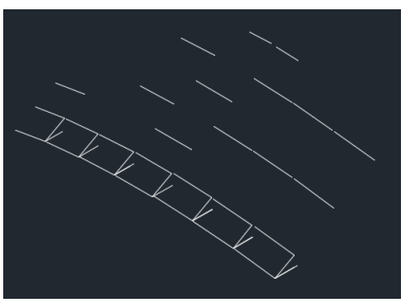

Figure 5 Drawing in autocad for the calculation of the azimuth
Source: Own elaboration

The same procedure is repeated for every section of the PV array. To check that the angle remained the same for the five elements, the same measurement was made in the different panels of each section. Table 2 shows the values of inclination and azimuth angle of each of the sections.

Section	Inclination	Azimuth
1	27.062°	351.14°
2	27.167°	354.16°
3	27.306°	356.90°
4	27.445°	0
5	27.584°	3.09°
6	27.700°	5.81°
7	27.823°	8.85°

Table 2 Inclination and azimuth angles for each section, own elaboration
Source: Own elaboration

Electrical characteristics

The 35 photovoltaic panels are made of polycrystalline silicon, Conergy brand P230PA model. The modules have a nominal power of 230 Wp under standard test conditions (STC, Standard Test Conditions) (Conergy, 2011). The system also has a microinverter for each panel for the conversion of electric power from DC to AC. These devices are of the Enphase brand M 190 72 240 model, with a conversion efficiency of 95%. The 35 modules are connected in parallel. The installation has a nominal capacity of 7.2 kW AC. The PV system is equipped with a data acquisition system. The inverters have a logic card that monitors the amount of energy produced and can transmit the information to a hub. This uploads the information to a database that can be reviewed online, on the manufacturer's website, Enphase Enlighten. Figure 6 shows a basic schematic of a photovoltaic solar system with an Enphase data acquisition system, which represents the study scenario in this paper.

Figure 6 PV system and data acquisition, Enphase energy.

The elements that allow the acquisition of data are presented below:

1) Microinverter that is responsible for the conversion of DC energy produced by the photovoltaic panels to AC to be consumed or transported to the network.

ISSN-2523-2517

2) Wiring that transmits the AC electrical energy converted by the inverters to a load center, and the production data signal.

3) Envoy data acquisition card that is responsible for uploading the information to the web page.

4) Router or modem to provide Internet connection.

5) Information system hosted on Enphase Enlighten's website.

This data acquisition system allows for a greater degree of confidence in the measurements made, since it avoids human errors in measurement and taking results.

Performance evaluation

Power production analysis

In this section an analysis of the electrical energy production of the modules is carried out according to their orientation, and for each of the panels. This analysis is based on radiation data provided by the RETScreen software and on solar radiation measurements made during the month of June on the University of Calgary campus.

In this study, the amount of energy produced by the panels daily is compared with the amount of solar energy they receive or average daily incident irradiance for the month of June 2014. The following method is applied in the analysis:

1) The daily average radiation is calculated using RETscreen, for each of the sections.

2) An energy production report is prepared for the month of June 2014, from the inverter's data acquisition system.

3) A table is made showing the production of the panels, average incident irradiance and the conversion efficiency (the latter is calculated taking the information of the production of the panels and the incident irradiance).

4) The efficiency obtained is compared with the nominal efficiency indicated by the manufacturer.

5) Steps one through four are repeated but using data from the University of Calgary Weather Station (WRS).

Method using RETScreen

RETScreen allows the analysis of different types of renewable energy projects. To start using it, the type of system to be analyzed is configured. Figure 7 shows the main RETScreen window, it shows the type of project, the application, the type of analysis, etc. These values are predetermined for each type of project, the current analysis project corresponds to a photovoltaic energy system.

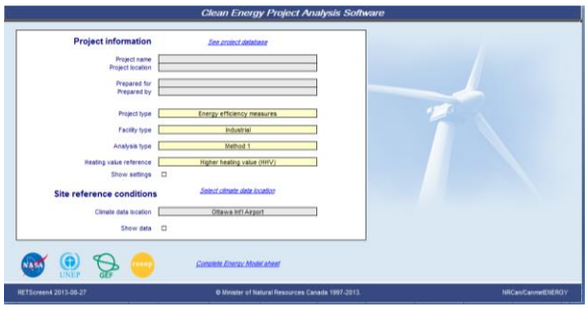

Figure 7 RETScreen main window
Source: Own elaboration with RETScreen.

To configure the analysis project, click the See Project database option, opening a dialog box (see figure 8) in which the following parameters are selected: Project type: Power; Type: Photovoltaic; Project name: 100 kW. Subsequently, click on the confirm button, which returns to the main window, but now shows the values of the selected project. Next, the local climate is selected (RETScreen has climate values from different parts around the world). A point is searched for and selected in the city of Calgary, which opens a new dialog box (see figure 9).

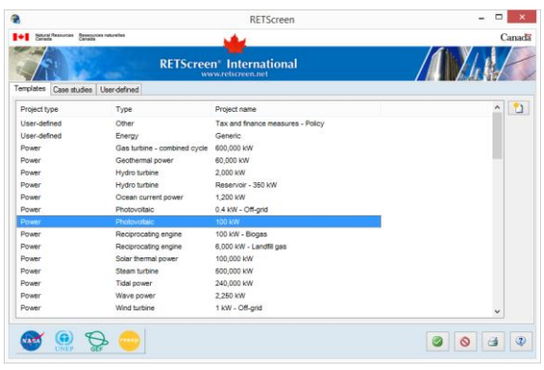

Figure 8 RETScreen window to select the project
Source: Own elaboration with RETScreen.

In this window, the location parameters to determine the meteorological values are selected. For the city of Calgary, there are values for the international airport, therefore, the parameters to be selected are the following:

- Country – región: Canada
- Province / State: Alberta
- Climate data location: Calgary Int'l. Airport

When selecting those parameters, the values corresponding to the international airport of the city of Calgary, a place very close to the University, are established.

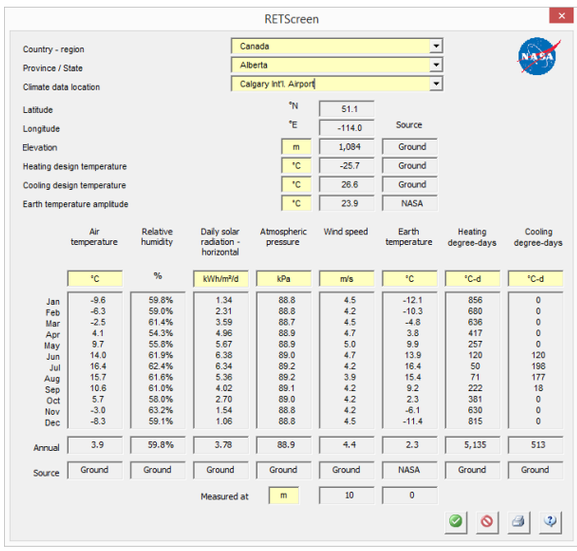

Figure 9 RETScreen window for locality selection, Own elaboration with RETScreen.

Of the values obtained in this table, the values for the month of June, the month for which the analysis is being carried out, are highlighted. For this month there are global and historical values of average radiation on a horizontal flat surface of 6.38 kWh/m^2/day, which is equal to 6380 Wh/m^2/day. The radiation values that are obtained are for horizontal surfaces; however, the study surfaces are not all horizontal. Due to the above, it is necessary to carry out the calculations for the average radiation for inclined surfaces. The advantage of this software is that it already has a programmed method. To calculate the radiation from inclined surfaces, click on the main window on Complete Energy Model Sheet, which is located at the bottom. This opens a tab of the program in which it is necessary to select method two, since it is the one that is programmed for this calculation.

For this method, it is necessary to introduce three parameters, one of them is the system tracking method, which in this case, being a fixed system, is selected as fixed. The other two parameters to set are the inclination and the azimuth for each panel or for each section. The angle values used are those shown in table 2. As an example, the calculations for section 1 are carried out with the following parameters:

1) Solar tracking mode: Fixed
2) Slope: 27.1
3) Azimuth: 351.1

The result, for all the sections corresponding to the inclined surface for the month of June, is shown in Table 3. The analysis for each section is made on this value.

Section	Irradiation (I) (kWh/m^2/day)
1	6330
2	6320
3	6320
4	6320
5	6320
6	6310
7	6310

Table 3 Irradiation results per section with RETScreen
Source: Own elaboration

Knowing the irradiation that reaches each one of the panels, a comparison can be made of the electric energy produced against the solar energy that it receives. For this, it is necessary to use the generated energy data saved on the server of the Enphase Enlighten website. The procedure, to calculate the average production of the panels for the month of June, consists first in downloading the total production data for each day of the month. Subsequently, the average for the 30 days of the month is obtained. This is achieved for each module. Although there is another factor to consider for this calculation, such as the area of the modules. From Table 3, an effective area of 1.65 m^2 (Conergy, 2011) must be considered to obtain the total radiation that reaches the modules. The efficiency (η) is calculated as the ratio between the average daily electrical energy production ($\bar{E}_s$) and the average solar energy ($\bar{E}_d$) that affects the modules during the month of June.

$$\eta = \frac{\bar{E}_d}{\bar{E}_s} \quad (1)$$

ISSN-2523-2517

The $\bar{E}_d$ is calculated by subtracting 5% of the measured energy from the inverter output. The $\bar{E}_s$ is calculated by multiplying the irradiation value (I) of the corresponding section (table 3) by the effective area (A_e) of the modules, this is done for each section.

$$\bar{E}_s = \mathrm{I} \times A_e \quad (2)$$

Method using WRS

The data provided by RETScreen are also an average of historical data from different databases, such as NASA, the departments of ecology of Canada and the United States, mainly. That is why the obtained results are lower than expected. For this reason, the study is also carried out, but using data that was measured in the field.

The irradiation data provided by the WRS are direct radiation values on a horizontal surface, distributed in 1-min intervals; therefore, it is necessary to average them per day and then per month to assess the daily production that the modules had during the month of June. The average radiation value according to the data was 5647.79 Wh/m^2, which is less than the value found in the RETScreen database by approximately 800 Wh/m^2. From this point it can be inferred that the efficiency of the modules is a little above what was measured previously. Based on the values obtained, the ratio of radiation that reaches the inclined surface to that which reaches the horizontal surface is calculated. The resulting ratio is called the radiation factor (RF), unique for each section. Table 4 shows the RF results.

Section	RF	Irradiation (kWh/m^2/day)
1	0.992	5603.52
2	0.990	5594.67
3	0.990	5594.67
4	0.990	5594.67
5	0.990	5594.67
6	0.980	5585.82
7	0.980	5585.82

Table 4 Ratio of inclined plane with the horizontal and irradiance by section
Source: Own elaboration

PVSYST

In (Project manual, 2011) they carry out a simulation study using PVSyst. Based on this information provided in their study, it follows that the efficiency of the photovoltaic array can be calculated from equation (3) and the results for the month of June are verified.

$$\mathrm{EffArrR} = \frac{EArray}{GlobInc \times Area} = \frac{1238kWh}{190\frac{kW}{m^2} \times 61.05\ m^2} \quad (4)$$

Where (in accordance with their terminology): EffArrR is the efficiency of the PV array; EArray is the received energy in the PV array; GlobInc is radiation factor and area is the area of the PV panel. For the month of June, it gives a result of EffArrR = 10.67 %.

Results and discussion

Firstly, a section is presented where the results obtained with the two methods seen (WRS and RETScreen) are presented and compared. Subsequently, in a following section, the comparison with the PVSyst results is performed.

WRS vs RETScreen comparison

The first comparison that is made is that of efficiency, but graphs are also analyzed where the energy received, and the energy produced per module per section are broken down.

PV modules efficiencies

Graphic 1 shows the efficiency results, in percentage, obtained with the WRS procedure. It is observed that the efficiency increases as the position of the panels is located further to the East, according to their corresponding section (table 2).

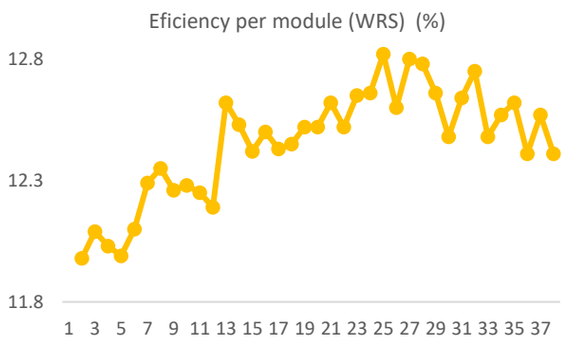

Graphic 1 Efficiency per PV module (WRS procedure)
Source: Own elaboration

On the other hand, graphic 2 shows the results of average efficiency per module section, for both procedures (WRS and RETScreen). For both methods, a profile can be observed where there is a tendency to increase the efficiency of the modules of the sections further east.

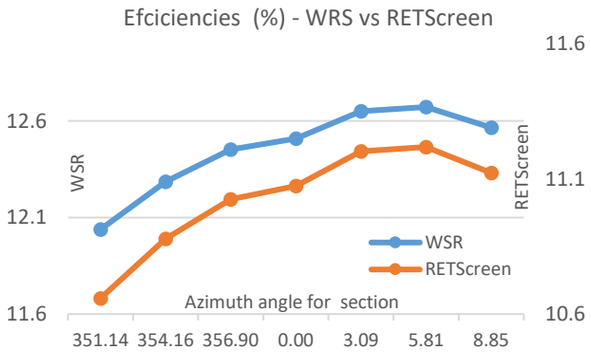

Graphic 2 Average efficiency per section (WRS and RETScreen procedure)
Source: Own elaboration

Received energy vs produced energy by the PV modules

An interesting exercise is to carry out the breakdown of the energies considered in the calculation of efficiency. In this way, graphic 3 shows the results of the energy received on average for each section of the module set. That information is shown for both methods (WRS and RETScreen).

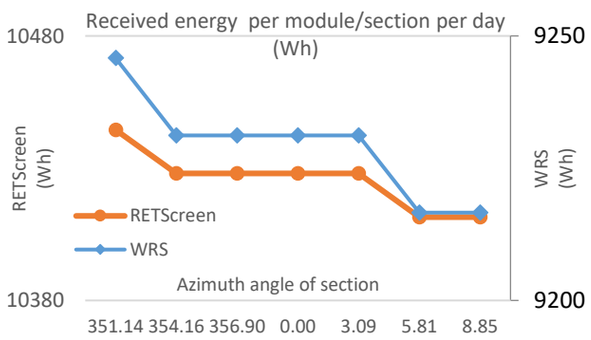

Graphic 3 Average received energy per section of PV modules for both methods (WRS and RETScreen)

From graphic 3, the results obtained for energy received using the method that involves the use of WRS data are lower (scale on the right) compared to those obtained by the method where the information is used. from RETScreen (scale on the left). On the other hand, a general trend can be seen in which the modules that receive more energy are those located in the sections further to the West.

According to graphic 2 and graphic 3, it can be commented that a behavior with a tendency to be inversely proportional is observed, where the sections that receive more energy are those that produce less. Given the above, the curves of energy received against energy produced are plotted, for the RETScreen and WRS method. These curves are presented in graphic 4 and graphic 5, respectively.

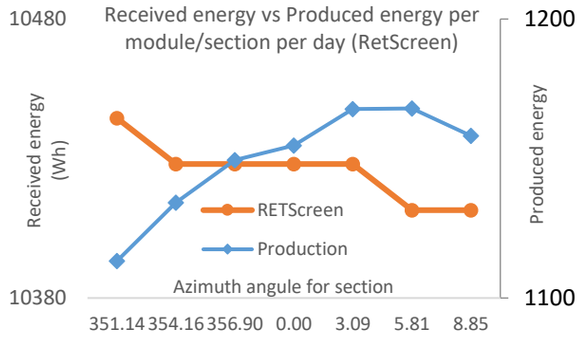

Graphic 4 Received energy vs energy produced per module (RETSCreen)
Source: Own elaboration

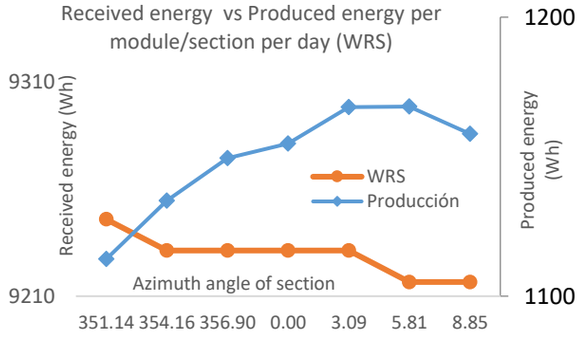

Graphic 5 Received energy vs produced energy (WRS),
Source: Own elaboration

From graphic 4 and graphic 5, the highest efficiency can be seen with the WRS procedure, where for a certain amount of received energy, the energy production is greater, observing a more efficient conversion capacity. The other interesting behavior is the one that has been observed in the sense that an inverse relation in the energy conversion. This is very noticeable in graphic 4, where the westernmost sections receive more solar energy, but produce less (left of the graph), while the easternmost sections receive less solar energy, but have a higher production (right of the graphic). Clearly, these behaviors are due to various factors, one of which may be the effect of the temperature of the panels on the conversion efficiency.

ISSN-2523-2517

Comparison with PVSYST

The average efficiency results obtained with the WRS and RETScreen methods are then compared with the efficiency value obtained in (1) with PVSyst. In addition, the nominal efficiency of the PV modules (Datasheet) is placed.

PVSyst	RETScreen	RWS	Maximum nominal efficiency
10.67 %	11.03 %	12.46 %	13.9 %

Table 5 Average efficiencies for the month of June
Source: Own elaboration

In the case of the efficiency obtained from RETScreen, it is quite close to the value obtained with PVSyst in the previous study. This would indicate that both simulators tend towards a very similar value. However, these are values that tend to be conservative in magnitude. The most accurate value is considered to correspond to the efficiency obtained from the WRS information, where the efficiency value is higher than in the case of the simulators.

Acknowledgment

To Dr. David Howe Wood of the University of Calgary, and to the Weather Station of the same university. This work has been partially financed with resources from the Autonomous University of Sinaloa, under the International Scientific Summer stay program in its VIII edition.

Conclusions

The electrical energy conversion performance of a photovoltaic array is evaluated. For the evaluation, the RETScreen software (free software from the Canadian government) was used to analyze the average efficiency of the panels for a month. An evaluation was also made with radiation values measured on the campus of the University of Calgary, which allowed obtaining greater precision and very similar results with a small difference of approximately 0.6%, so the data delivered by this software is very reliable and serve to make projections with a small error. In the results it can be observed that the panels of sections 5-6 had a higher yield (approximately 0.5%).

Making a comparison between the modules that produced more energy and those that produced less, it was found that those that were facing east had the best yields with an average difference of 0.6% more than those that were oriented to the west, the equivalent of approximately 60-65 Wh and which allows a fluorescent bulb to be on for 5 hours.

References

Bueno Rivera, R. (2015). Análisis del impacto de la temperatura y orientación en el rendimiento de un sistema fotovoltaico (Tesis de Licenciatura). Universidad Autónoma de Sinaloa. Ingeniería en procesos industriales. Culiacán, Sinaloa. México. https://drive.google.com/drive/folders/1-lcRJ6DD2PnpjtooGH1yfF6aAl9DvUVR

Conergy. (2011). Conergy P 220PA-240PA. Specifications Photovoltaic modules. https://www.enfsolar.com/Product/pdf/Crystalline/50498ccd4c56a.pdf

Jena, R., Dash, R., Reddy, K. J., Parida, P. K., Dhanamjayulu, C., Swain, S. C., & Muyeen, S. M. (2023). Enhancing Efficiency of Grid-Connected Solar Photovoltaic System with Particle Swarm Optimization & Long Short-Term Memory Hybrid Technique. *Sustainability*, *15*(11), 8535. https://www.mdpi.com/2071-1050/15/11/8535 https://doi.org/10.3390/su15118535

Galicia, R. H., Alegría, A. S., Sol, Á. H., López, Á. G., & López, A. A. D. (2023). Correlation between the efficiency of a solar panel and the environmental conditions by the multiple linear regression method for the city of Tuxtla Gutierrez. *Pistas Educativas*, *44*(144). https://pistaseducativas.celaya.tecnm.mx/index.php/pistas/article/view/2934/2285

Kahar, N. H. A., Azhan, N. H., Alhamrouni, I., Zulkifli, M. N., Sutikno, T., & Jusoh, A. (2023). Comparative analysis of grid-connected bifacial and standard mono-facial photovoltaic solar systems. *Bulletin of Electrical Engineering and Informatics*, *12*(4), 1993-2004. https://beei.org/index.php/EEI/article/view/5072/3292 https://doi.org/10.11591/eei.v12i4.5072

Manas, M., Dakka, O., Sharma, S., Arandhakar, S., Kallelapu, R., & Golla, S. (2023). A novel metaheuristic-based robust unified control MPPT algorithm for grid-connected PV system. *Electric Power Systems Research*, *221*, 109389. https://www.sciencedirect.com/science/article/pii/S037877962300278X https://doi.org/10.1016/j.epsr.2023.109389

Song, Y., Mu, H., Li, N., & Wang, H. (2023). Multi-objective optimization of large-scale grid-connected photovoltaic-hydrogen-natural gas integrated energy power station based on carbon emission priority. *International Journal of Hydrogen Energy*, *48*(10), 4087-4103. https://www.sciencedirect.com/science/article/pii/S0360319922047905 https://doi.org/10.1016/j.ijhydene.2022.10.121

Team Canada. (2011). Project Manual - TRTL: Technological Residence, Traditional Living. Solar Decathlon. University of Calgary. Alberta, Canada. https://www.solardecathlon.gov/past/2011/pdfs/canada_manual.pdf

ISSN-2523-2517

Article **Journal Electrical Engineering**
December 2023, Vol.7 No.19 25-37

Energy and exergy analysis at the la joya sugar mill in Champotón, Campeche, Mexico

Análisis energético y exergético en el ingenio azucarero de la joya en Champotón, Campeche, México

CHAN-GONZALEZ, Jorge J.†, CASTILLO-GAMBOA, Andrea, LEZAMA-ZÁRRAGA, Francisco* and SHIH, Meng Yen

Universidad Autónoma De Campeche, Campus V, Predio s/n por Av. Humberto Lanz Cardenas y Unidad Habitacional Ecologica Ambiental, Col. Ex-Hacienda Kala, CP 24085, San Francisco de Campeche, Cam., México.

ID 1st Author: *Jorge J., Chan-Gonzalez* / **ORC ID:** 0000-0002-8638-1646, **CVU CONAHCT ID:** 89415

ID 1st Co-author: *Andrea, Castillo-Gamboa* / **ORC ID:** 0009-0002-7179-4824

ID 2nd Co-author: *Francisco, Lezama-Zárraga* / **ORC ID:** 0000-0001-7475-6458, **CVU CONAHCT ID:** 205493

ID 3rd Co-author: Meng Yen, Shih / **ORC ID:** 0000-0001-7475-6458, **CVU CONAHCT ID:** 408617

DOI: 10.35429/JEE.2023.19.7.25.37 Received July 20, 2023; Accepted December 30, 2023

Abstract

An energy and exergistic analysis was carried out on the bagacera boiler of the sugar mill "La Joya" located in Champotón, Campeche, making the following assumptions: the process develops in a permanent state, the mass that flows through the control volume does not suffer variations with respect to time, there are no work interactions of the system with the environment, changes in kinetic energy and potential energy are considered negligible, thermodynamic data were provided by the mill's operation and control center. It was found that by increasing the mass flow of feed water (m_{water}) and decreasing the temperature of the dead state (T0) there was the least destruction of exergy. Simulations were carried out to determine the energy and exegetical efficiencies of the mill as a whole with the help of the Software Engineering Equation Solver (EES). When modifying $\dot{m}\_water$, with T0 at 25 ℃, and inlet water (T_{water}) 90 ℃, an increase was observed both efficiencies; the energetic reached a maximum of 88, and the exergetic of 31; It was also observed that the maximum energy efficiency is obtained with the Twater 45℃. On the contrary, the exergetic efficiency at 15.3. It was concluded that it is more important to increase the mass flow of inlet water to increase global efficiencies in mill facilities than its temperature.

Energy and exergetic analysis, energy and exergetic efficiencies, bagasse-based cogeneration plant, sugarmill

Resumen

Se realizó un análisis energético y exergético sobre la caldera bagacera del ingenio azucarero “La Joya” situado en Champotón, Campeche, haciendo las siguientes suposiciones: el proceso se desarrolla en estado permanente, la masa que fluye por el volumen de control no sufre variaciones con respecto al tiempo, no hay interacciones de trabajo del sistema con el medio ambiente, los cambios en la energía cinética y la energía potencial son considerados como despreciables, los datos termodinámicos fueron proporcionados por el centro de operación y control del ingenio. Se encontró que aumentando el flujo másico del agua de alimentación ($(\dot{m}_{agua})$) y disminuyendo la temperatura del estado muerto (T0) se tuvo la menor destrucción de exergía. Las menores temperaturas del estado muerto sólo se tienen para la época de otoño-invierno. Con la disminución del flujo másico del agua de alimentación, el precalentamiento de la misma antes del ingreso a la caldera y la T0 más baja posible se logró la menor destrucción de exergía. Se realizaron simulaciones para determinar las eficiencias energéticas y exegéticas del ingenio en su conjunto con la ayuda del Software Engineering Equation Solver (EES). Al modificar $\dot{m}\_agua$, con T0 en 25 °C, y agua de entrada (T_{agua}) 90 °C, se observó un aumento ambas eficiencias; la energética alcanzó un máximo de 88, y la exergética de 31; también se observó que la máxima eficiencia energética se obtiene con la Tagua 45 °C. Por el contrario, la eficiencia exergética a 15.3. Se concluyó que es más importante aumentar el flujo másico del agua de entrada para aumentar las eficiencias globales en las instalaciones de un ingenio, que la temperatura de la misma.

Análisis energético y exergético, eficiencias energética y exergética, cogeneración en caldera bagacera, ingenio azucarero

Citation: CHAN-GONZALEZ, Jorge J., CASTILLO-GAMBOA, Andrea, LEZAMA-ZÁRRAGA, Francisco and SHIH, Meng Yen. Energy and exergy analysis at the la joya sugar mill in Champotón, Campeche, Mexico. Journal Electrical Engineering. 2023. 7-19:25-37.

* Author's Correspondence (E-mail: frlezama@uacam.mx)
† Researcher contributing as first author.

Introduction

In the context of Mexico's energy development, the "La Joya" sugar mill located in the municipality of Champotón, Campeche, Mexico, acquired a 20 MW turbo mega generator (TMG). Mexico, acquired a turbo mega generator (TMG) with a capacity of 20 MW. To date, it is fully installed. The purpose of this generator was to increase the company's own production of electricity and minimize the consumption of energy from the Federal Electricity Commission (CFE) network. The start-up of the TMG revealed a reality different from what was foreseen; the parameters of the steam produced by the baghouse boiler were not able to sustain the efficiency and production of the TMG. This implied making improvements in the steam production; therefore, an analysis of the boiler was proposed to determine if its production was sufficient and of the required quality. Most baghouse boilers in the world operate with technology from the beginning of the last century. Sugar production requires high-temperature processes obtained with steam or hot water; they are used for cleaning, evaporation and cooking of the sugarcane juice. In the early days of sugar production, firewood was used for the cooking processes; this fuel was a concern for landowners and administrators because the costs were onerous. Some time later (1647), sugarcane bagasse began to be used as fuel (Rivero, R. and Anaya, 1986). The introduction of steam in this industry occurred for the first time in Jamaica in 1768 in the Greenwich plantation, and was due to a John Stewart patent on the design of transmission of the energy produced by a steam engine to a sugar cane mill (Hugot, 2011). The first successful application of steam in mill and transmission processes was made in Cuba in 1797 at the estate of the Count of San Juan de Jaruco in Seibado; by 1808 there were already 25 mills operating with this type of energy (Molina Lóp ez, 2015). The old boilers were manufactured in three levels. Only the lower one was made of a single piece of metal, while the others were made of plates bolted or riveted together. This facilitated the replacement of the bottoms, the parts that wore out the most when exposed to the heat of the direct fire applied to them. The material used in their manufacture was copper; by 1880 some boilers were made of copper and bronze alloy, which made them lighter (Ruiz Labourdette, 2012).

It was not until the end of the 19th century that cast iron began to become widespread (Thomasset, 2011) for the manufacture of boilers. Innovations in boilers were subject to the conditions of the economic and social environment of the time. As new proposals were made, these boilers were used to generate electric power by coupling a turbine to an electric generator (Vallejo, 1982). The first electric power generators driven by steam generation were built, converting thermal energy into motion and motion into electric power generation (Molina López, 2015).

The bagasse boiler

This type of boiler is called bagasse due to the characteristic of its combustion, which uses bagasse (which is considered waste or garbage) as its raw material and converts it into fuel, Figure 1. The bagasse is transported by long belts and inserted into a furnace where combustion takes place, which heats the water supplied, until the necessary steam is obtained, which drives the turbine and propitiates the generation of electric energy through the electric generator coupled to the turbine. The furnaces of these boilers have adjustments in the arrangement of the bagasse supply, and a special ash removal system, as well as burners suitable for this fuel (Pistore, 2012).

Figure 1 La Joya sugar mill baghouse boiler
Source: Own elaboration.

ISSN-2523-2517

The first bagasse boilers were used to obtain sugar in haciendas that followed a traditional process. Sugar production was carried out with traditional implements in three distinct stages:

1. The sugar mill, where the milling process was carried out.

2. The boiler house, where there was a battery of kettles, pots, pots and cauldrons, which produced the heat necessary to carry out the processes of cleaning, evaporation and cooking of the sugar cane juice; these utensils could be said to be the first bagasse boilers. Later on, the essential equipment in this sector of the sugar mill was the set of vessels and cauldrons where the successive boiling heats of the guarapo were carried out, complemented by some scarce instruments for the manipulation.

3. The purging, where the crystallized sugar was separated from the honeys (Shield, 1975).

Nowadays, boilers are built with a high technological level, Figure 2, which achieve high yield results, all this added to the knowledge we have about the properties of water and steam.

Figure 2 Top view of the dome of a modern bagasse boiler
Source: Own elaboration

It is also noteworthy the great progress achieved in metallurgy; it has allowed the use of steels and alloys that withstand both, higher pressures and high temperatures; materials that also resist corrosion significantly (Manso, W. and Castillo, 2015).

Currently, the standards (NFPA 85-2019 and NOM-122-STPS-1996) that regulate the design and construction of steam boilers must be complied with, allowing control over the critical parts of these, which also helps to have better safety levels (Tornero, 2011). However, although the development of boilers is much and their manufacturing has been improved, sugar mills are characterized for being highly energy consuming and wasteful; largely due to low efficiency technology, as well as to the neglect of their facilities. Specifically, in sugar mills; steam generators are little attended as carriers of improvement in the production and performance of the same despite the fact that their operation involves the conversion of the energy potential of bagasse into thermal energy which in turn performs the transmission of this energy to a medium (steam), which can be used in useful work both in the industrial manufacturing process and for mechanical work of turbogenerators and mills (Ramos et al., 2019). While modern boilers are becoming more prevalent in new projects, there remains a large majority of older equipment that needs to be repowered (Singh, 2019). A boiler is itself an assembly, containing different elements (Ruiz Labourdette, 2012). Figure 3 shows a scheme that visualizes the points where bagasse, air and water involved in steam production are injected:

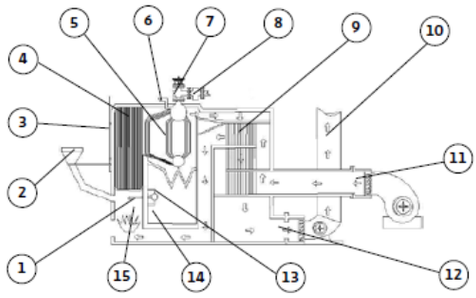

Figure 3 Main components of bagasse boiler
Source: Tornero et al., 2011

1 Burner	9 Air preheating
2 Bagasse Feeder	10 Chimney
3 Water level	11 Forced air duct
4 Fluxeria	12 Induced air duct
5 Steam overheating	13 Fuel oil spraying pipe (auxiliary)
6 Water inlet	14 Fuel oil pipe (auxiliary)
7 Steam outlet valve	15 Home
8 Steam non-return valve	

ISSN-2523-2517

Justification

This work consisted of applying the exergetic method in the processes or stages developed at "La Joya" sugar mill, particularly in the bagasse boiler, to achieve maximum steam production under optimum operating conditions, according to the technical sheet of a 20 MW Turbo Mega Generator (TMG). With data provided by the Mill's Production Department, the production and management of operating steam in a month for the industrial process and electric power generation was determined, as shown in the monthly summary in Graph 1.

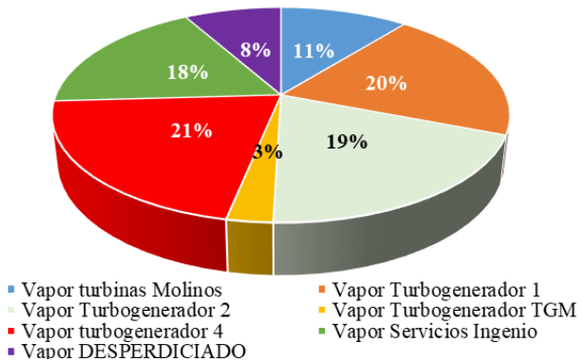

Graphic 1 Percentage of steam consumption at sugar mill Joya, Champotón, Campeche, Mexico
Source: Own elaboration.

Steam production in the boiler was 24.33 kg/s, of which 21.81 kg/s were used throughout the industrial process (auxiliary services steam) and for electricity generation. The mill estimated an approximate loss of 2.52 kg/s (this steam may have escaped at joints, pipes and valves). Although it appeared that they had excess steam, the reality is that it was not injected to the TMG in the quantity and quality necessary for the proper operation of the turbogenerator. It was necessary to increase the quantity and check the conditions of the steam to the TMG. With the steam in the initial conditions, it was impossible to sustain the production of electrical energy from the TMG (tripping). The conditions required by the TMG datasheet are as follows: Steam injection temperature 350 °C. Operating pressure 3.5 MPa (superheated steam conditions). Graph 1 shows that only 29% (Molinos turbines 11% and Ingenio Services 18%) of the steam was used directly in the industrial process, and 63% was used in electricity generation in 4 different types of generators. In addition, 8% of steam (purple tone) was not used in any part of the process.

It is possible to present different proposals to increase steam injection to the TMG:

– Change of equipment and auxiliary devices that are obsolete and decrease the steam production capacity.

– Change in pipes, fittings and valves in bad conditions or improve their quality.

– Exergetic and energetic analysis and redesign of the thermodynamic cycle used.

The boiler is the place of maximum energy loss (by the amount of heat lost), but also the place of thermal energy creation, the focus of this work was to demonstrate that, by enhancing the efficiency of the heart of the plant, the operating efficiency of the system as a whole is increased.

Objective

To achieve the maximum steam production in a steam generator (baghouse boiler) of a sugar mill, at the optimum operating conditions, according to the technical sheet, of the TMG of 20 MW, determined through the application of energy and energy analysis to the industrial process and electric power generation of the sugar mill in operation. As well as to contribute with low investment energy strategies,

Hypothesis

A fundamental parameter for the steam production of the boiler is the nominal power of the Turbo mega Generator. This power is ideal, it is not attached to the real power of the system. The manufacturer does not consider losses and irreversibilities; in specific climatic and geological situations there are important variations with the values according to the working place of the equipment. With the application of the exergy method, the optimal operating conditions of the baghouse boiler and the losses in strategic points, which cause its low efficiency and poor steam quality in the system, will be determined.

ISSN-2523-2517

Problem Statement

The mill is operated with a steam generator, fed with sugarcane bagasse (bagasse boiler). The generator produces superheated steam which is injected into the turbine of the 20 MW electric generator (TMG). However, during the operation of the TMG the plant was experiencing failures or tripping of the steam line feeder valves, leaving the turbine out of service; after reviewing the system and its operation, it was determined that the steam did not meet the specifications (quality) demanded by the technical sheet of the TMG electric generator. Therefore, the problem to be solved was to obtain and improve the quality of the steam required for the optimal operation of the TMG. According to the TMG data sheet, the required steam conditions (parameters to be met) were determined for this purpose. The analysis of the baghouse boiler was proposed to improve its production and efficiency. We pointed out that, even limiting the analysis to the boiler, there were problems in the equipment or processes. It was proposed to solve these problems with:

– Replacement of obsolete equipment that reduces the capacity and quality of steam production.

– Change in current piping, accessories and valves to others of higher quality.

– Analysis and redesign of the thermodynamic cycle used. In first and second law**.**

This project proposed to increase the efficiency of the baghouse boiler to supply optimum steam to the 20 MW turbogenerator. Also, it was proposed the energetic and energetic analysis applied to the steam generator, to identify which are and how the maximum losses occur in it. In this way to avoid costly investments, which have little impact on the good performance of the system (Ma *et al.*, 2023).

Methodology proposed for the analysis of the baghouse boiler

An energetic and energetic analysis was carried out on the steam generator (baghouse boiler). According to the literature review, several authors highlight that, within a traditional sugar mill, the steam generation area presents the main energy losses with 53.3% (Molina López, 2015). However, all these designs are based on technical-economic criteria from the point of view of the first law of thermodynamics and although the determining factor of efficiency is the fuel converted to energy, it is advisable to perform the energetic balance. Therefore, the energetic analysis of the baghouse boiler and its relationship with the whole cycle as a whole was developed in order to establish the best conditions under which it can operate more efficiently (Ma et al., 2023). We start for this analysis, the current operating conditions. The steam generator analysis was performed under the following thermodynamic assumptions:

– The process runs in steady state.

– The mass flows through the control volume; it does not undergo variations with respect to time, therefore, the variation of this is equal to zero.

– By balance, the Enthalpy and Entropy difference must be equal to zero.

– There are no work interactions of the system with the environment (no arrow work).

– Changes in kinetic energy and potential energy are considered negligible.

– The thermodynamic data for each point were obtained from the La Joya mill's operation and control center during normal operation.

ISSN-2523-2517

Theoretical framework

Under the above assumptions, the mass and energy balances for this system can be expressed as a ratio as follows: steam generator (baghouse boiler): mass, energy and exergy balances for the control volume. For a steady state control volume with negligible changes in kinetic and potential energies, the mass, energy and exergy balances are as follows (Cengel, 2015),(Cengel, 2011):

$$\sum\left(1-\frac{T_0}{T}\right)\dot{Q}-\dot{W}+\sum c\psi_{output}-\sum\dot{m}_{input}\psi_{input}-\dot{X}_{ddestroyed}= \quad (1)$$

$$\left(1-\frac{T_0}{T}\right)\dot{Q}-\dot{W}+\dot{m}_{\dot{m}_{output}}(\psi_{input}-\psi_{einput})-\dot{X}_{destroyed}=0 \quad (2)$$

Being:

$\dot{m}$ mass flow rate of the process water or steam.
$\dot{Q}$ process heat
$\dot{W}$ arrow work
h enthalpy of a specific point
$\dot{X}_{destroyed}$ exergy destroyed.
ψ *exergy of a specific point.*

The thermal exergy transfer flux due to heat transfer from the boiler to the environment, at temperature T (expressed in K) is given by: : $\sum\left(1-\frac{T_0}{T}\right)\dot{Q}$. Where T_0 is the dead state temperature (room temperature expressed in K). The exergy of water and steam are given by the following equation:

$$\dot{m}_{fluid}(\psi_{output}-\psi_{input})=\dot{m}[(h_{output}-h_{input})]$$

$$-T_0(s_{output}-s_{input}) \quad (3)$$

Substituting Equation 3 into 2, the relationship for a steady flow device and a single current (one input and one output), is as follows:

$$\left(1-\frac{T_0}{T}\right)\dot{Q}-\dot{W}+m[(h_{output}-h_{input})-T_0(s_{output}-s_{input})]-\dot{X}_{destruida}=0 \quad (4)$$

For our case there is no arrow work so $\dot{W}$ is equal to zero. The energy efficiency of the plant is given by (Singh, 2019).

$$\sum\left(\frac{1-T_0}{T}\right)\dot{Q}-\dot{W}=\sum\dot{m}_{output}\psi_{output}-\sum\dot{m}_{input}\psi_{input}+\dot{X} \quad (5)$$

The total heat used in the sugar production process is given by:

$$\dot{Q}_{process}=\dot{Q}_{\text{boiler house}}+\dot{Q}_{miscellaneus} \quad (6)$$

$\dot{Q}_{miscellaneus}$ = *negligible*

The energy efficiency of the plant is given by (Singh, 2019):

$$\eta_{energy\ plant}=\frac{\dot{W}_{net}+\dot{Q}_{process}}{\dot{E}_{combustión}} \quad (7)$$

$$\eta_{energy\ plant}=\frac{\dot{W}_{net}+(\dot{H}_{input}-\dot{H}_{output})}{10{,}276\frac{kJ}{kg}*\dot{m}_{combustible}} \quad (8)$$

The total exergy used during the sugar production process is (Kanoglu & Dincer, 2009):

$$\eta_{energy\ plant}=\frac{\dot{W}_{net}+\dot{X}_{process}}{\dot{X}_{fuel}} \quad (9)$$

The fuel exergy is given by:(Singh, 2019).

$$\psi_{fuel}=\psi_{fuel\ chemistry}=12{,}459\ \frac{kJ}{kg}$$

$$\eta_{energy\ plant}=\frac{\dot{W}_{neto}+(\dot{X}_{output}-\dot{X}_{input})}{12{,}459\frac{kJ}{kg}*\dot{m}_{fuel}\frac{kg}{s}} \quad (10)$$

$$\dot{X}_{output}=\dot{m}_{fluid}\psi_{input}=\dot{m}_{fluid}[(h_{input}-h_0)-T_0(s_{input}-s_0)] \quad (11)$$

$$\dot{X}_{output}=\dot{m}_{fluido}\psi_{input}=\dot{m}_{fluid}[(h_{output}-h_0)-T_0(s_{output}-s_0)] \quad (12)$$

$$\dot{W}_{net}=\dot{m}_{vapor}\frac{kg}{s}(h_{steam\ turbine\ output}-h_{steam\ turbine\ inlet})\frac{kJ}{kg} \quad (13)$$

The related properties in the specified states are determined by steam tables (Cengel, 2015) and EES own libraries. The "La Joya" sugar mill has an automated monitoring and control system (Computerized Command Center). It monitors in real time the main operating parameters, Figure 4.

ISSN-2523-2517

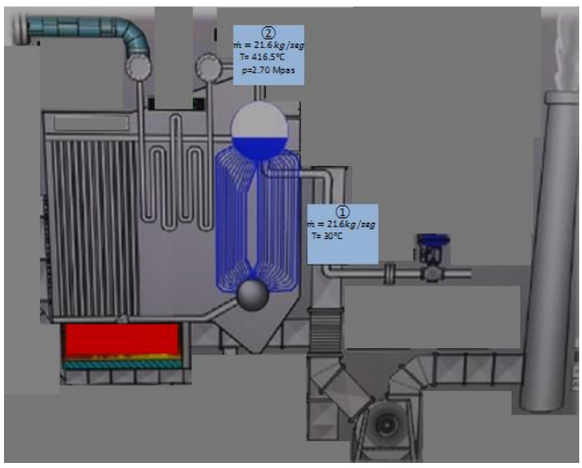

Figure 4 Diagram of the steam generator with its operating parameters
Source: La Joya mill computerized command center.

System operating data

The sugar mill's control system provided us with its operating data recorded and compiled during the harvest process, specifically for the steam generator (baghouse boiler). Figures 4 and 5, and Table 1. We used the Engineering Equation Solver (EES) software to determine the thermodynamic properties of these points, Table 1. A schematic diagram of the boiler was made as a control volume for analysis.

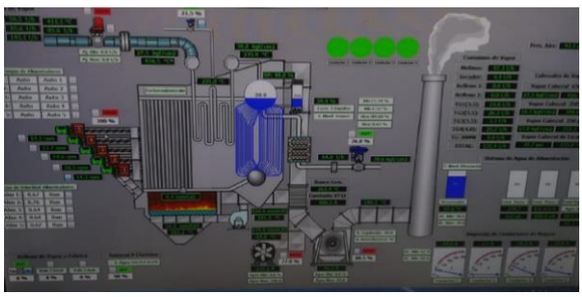

Figure 5 Diagram of the system analyzed in the steam generator
Source: Ingenio la Joya control system. Own elaboration

Figure 6 is the schematic diagram of the control volume of our analysis; the steam generator presented in a simplified form. It shows the mass flow of the feed water and the hearth. Steam production at 416 °C and 2.70 MPa is considered. The assumptions of the problem are the same as those stated above.

State	ṁ [kg/s]	T [ºC]	P [MPa]	h [kJ/kg]	s [kJ/(kg K)]
1	21.6	30	0.00424	125.74	0.4368
2	21.6	416	2.7	3272.64	7.0310

Table 1 Thermodynamic properties of selected points to perform the analysis
Source: La Joya Control Center.

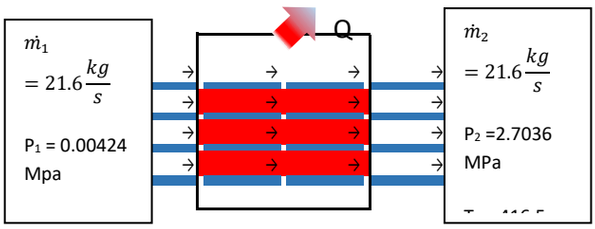

Figure 6 Schematic diagram of the control volume. Simplified shape of the steam generator
Source: own elaboration.

The assumptions of the problem are the same as those pointed out in previous paragraphs. The diagram allowed us to visualize that there was a problem in the quality of the steam obtained, since the requirements according to the technical specifications of the turbogenerator are: temperature and outlet pressure of the superheated steam 350 oC and 3.5 MPa respectively. The exergy destroyed is given by equations 1, 2 and 3 (Cengel, 2015):

$$\dot{X} = T_0 \, S_{generated} \quad (1) \quad (14)$$

$$\dot{S}_{generated} = \dot{m}_1 * (\dot{S}_1 - \dot{S}_2) \quad (2) \quad (15)$$

$$\dot{X}_{destroyed} = \left(1 - \frac{T_0}{T}\right) Q + \dot{m}[(h_1 - h_2) - T_0 \, S_{generated}] \quad (3) \quad (16)$$

Energy balance

For the proper operation of the integral system of the La Joya sugar mill, a steam mass flow was required at a temperature of 350 °C and a pressure of 3.5 MPa. On the other hand, the total steam produced by the mill before our analysis was 24.3 kg/s and wasted 2.6kg/s. It was proposed to increase the mass flow and steam quality to reach the required and adequate output conditions. Figure.3 represents the conditions required by the TMG data sheet. When comparing the diagrams in Figures 3 and 2, a difference in the outlet pressure (P_2) of 0.7 MPa is observed with respect to the condition in Figure 2. There is also a difference in the steam mass flow rate by 10 kg/s.

ISSN-2523-2517

Exergetic balance

Taking into account the above, it is proposed:

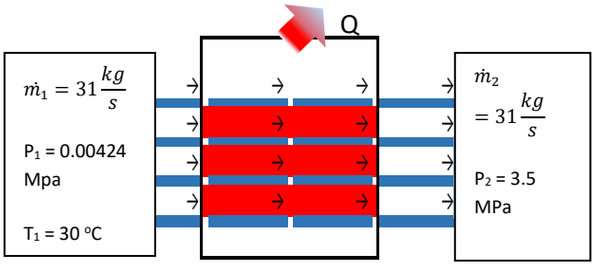

Figure 7 Schematic diagram of the control volume with the required values. Simplified shape of the steam generator
Source: own elaboration.

1. To produce steam to what is strictly necessary for the needs of the mill.

2. To consume the strictly necessary amount of steam. Fuel for the steam generator (sugarcane bagasse) is not a problem, it is in excess. There is a problem in the use of water needed for steam production. It requires extraction and subsequent treatment (softening it to convert it to steam). Therefore, it was proposed to focus on the efficient use and consequent saving of water in two ways:

   – Adjust the water temperature at the inlet to the steam generator and thus increase the efficiency of the system.

   – Adjusting the mass flow of the feed water to achieve greater system efficiency.

According to what was described in the previous paragraph, several simulations were carried out applying the equations previously described. We note that the inlet temperature of the feed water is a preponderant factor for the generation of entropy and the consequent destruction of exergy. Therefore, it is recommended that the boiler supply water be preheated before entering the boiler. This can be achieved if a water preheater is installed in the cycle; it will be necessary to check if this proposal is economically feasible. At different inlet temperatures, the behavior of the steam in entropy generated and exergy lost were calculated. Another way to save energy is to limit the mass flow of water.

Remembering that this is a necessity since it reduces water treatment costs (softening); for this analysis we used a mass flow rate of 16.6 kg/s. To complement this, a comparison is proposed at different possible dead state temperatures for Champotón, Campeche. The corresponding calculations were performed and the following results were obtained.

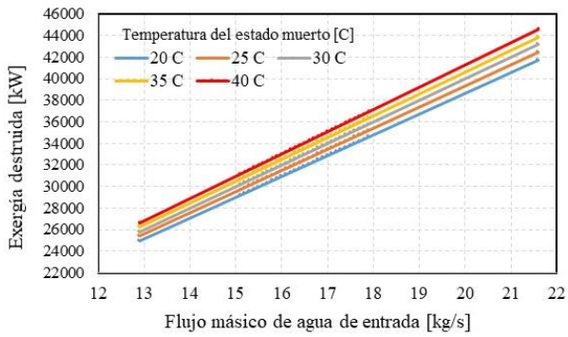

Graphic 2 Parametric analysis of the exergy destroyed as a function of the dead state temperature (T_0) and the feed water temperature in the baghouse boiler at a constant mass flow rate
Source: own elaboration

The exergy destroyed as a function of the dead state temperature (T_0) and feed water temperature in the baghouse boiler is observed. We note that the lower the dead state temperature (ambient temperature) and the higher the feed water inlet temperature, the lower the exergy destruction. However, the lower dead state temperatures are only for the fall-winter season and it is a parameter that we cannot control. On the other hand, the controllable parameter is the inlet water temperature. Parametric analysis of the variation of destroyed exergy as a function of the dead state temperature (T_0) and the mass flow rate of the feed water in the baghouse boiler was also performed. The results are presented in Graph 2. The variation of exergy destroyed as a function of the dead state temperature (T_0) and the mass flow rate of the feed water in the baghouse boiler is observed. It can be seen that the higher the mass flow rate of the feed water and the lower the dead state temperature (ambient temperature), the lower the exergy destruction. However, the lowest dead state temperatures are only available for the autumn-winter season and it is a parameter that we cannot control. The controllable parameter is the mass flow rate of the feed water to the baghouse boiler.

ISSN-2523-2517

From the previous graphs, 1 and 2, it is concluded: with the decrease of the mass flow of the feed water, and the preheating of the feed water before it enters the boiler and with the dead state temperature conditions as low as possible, the lowest exergy destruction is achieved. However, this exergy analysis is only performed for the steam generator or baghouse boiler. It is necessary to know the behavior of the sugar mill as a whole, to establish whether it is feasible or not to control the mass flows of the feed water, as well as its inlet temperature.

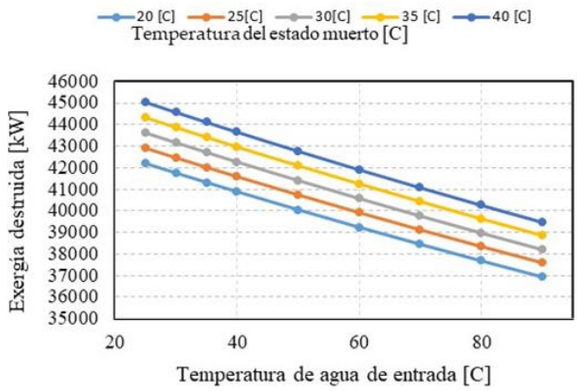

Graphic 3 Parametric analysis of the variation of exergy destroyed as a function of the dead state temperature (T_0) and the mass flow of the feed water in the baghouse boiler
Source: own elaboration

In addition, simulations were carried out by applying equations 1 to 13, to determine the energy and exergy efficiencies of the mill as a whole. The values provided by the mill's control center were used as input data. The Engineering Equation Solver (EES) software was used to perform the calculations. The programming done in EES is presented (report format) as well as the results obtained according to the proposed variations.

Algorithm written in EES, report format.

$$\eta_{energía} = \left[\frac{\dot{W}_{turbina} + \dot{m}_{agua} \cdot (h_{vapor} - h_{agua})}{10276 \cdot \dot{m}_{bagazo}}\right] \cdot 100$$

The results obtained are shown in Graphs 4a) and 4b). It is observed that the temperature of the water entering the steam generator is an important factor in the variation of the efficiencies (energetic and exergetic), however, its influence on the energetic efficiency is more important. When going from 25 to 50 ^oC, the energy efficiency changes by 2.5 units, while the exergy efficiency changes only 0.08 units.

In Figure 4a), a mass flow rate of 21.5 kg/s was maintained and the dead state temperature was kept fixed at 25 ^oC. For Graph 4b), a mass flow rate of 16.6 kg/s was maintained and the dead state temperature was kept fixed at 25 ^oC. We also note that the energy and exergy efficiencies decrease considerably as the mass flow rate of the supply water decreases. Both show that the energy efficiency decreases linearly as the boiler inlet water temperature increases; the exergy efficiency also shows a decrease, in a parabolic form, as the boiler inlet water temperature increases. Figure 5 shows the variation of the mass flow rate of the boiler feed water, keeping the dead state temperature (T_0) fixed at 25 ^oC, and the inlet water temperature (W_{ater}) at 30 ^oC, and the change of the energy and exergy efficiencies as it changes. We note that, in both cases, the efficiencies increase with increasing mass flow rate. The increase in energy efficiency is more noticeable when increasing the mass flow from 10 to 25 kg/s, there is an increase of 49 units with a maximum of 85, while in the exergy efficiency the change was only 15 units from 16 to 31.

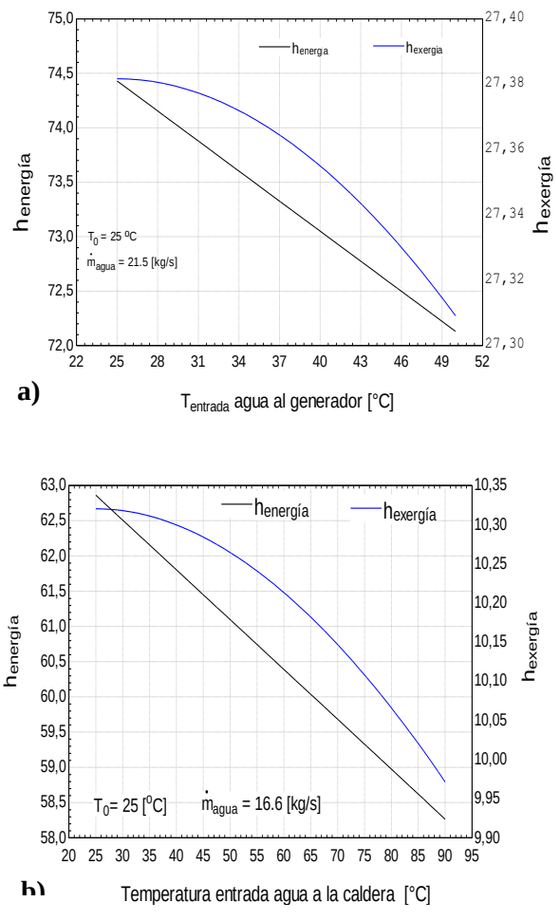

Graphic 4 Parametric analysis. Variation of the energy and exergy efficiencies of a sugar mill as a function of the temperature of the water entering the boiler and the mass flow of the feed water to the baghouse boiler
Source: Own elaboration

ISSN-2523-2517

In Graph 5 we observe the variation of energy and exergy efficiencies when the mass flow of the baghouse boiler feed water is modified, keeping the dead state temperature (T_0) fixed at 25 ºC, and the inlet water temperature (T_{water}) at 30 ºC. We note that, in both cases, the efficiencies increase as the mass flow rate increases. The increase in energy efficiency is more noticeable when increasing the mass flow from 10 to 25 kg/s, there is an increase of 49 units with a maximum of 85, while in the exergy efficiency the change was only 15 units from 16 to 31.

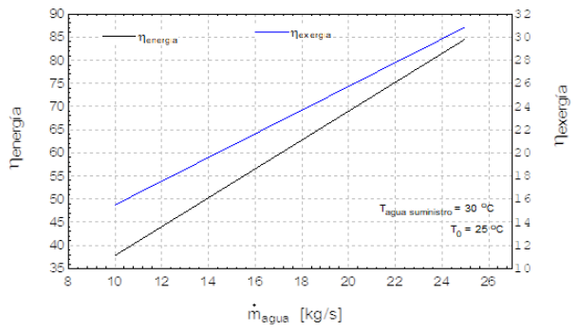

Graphic 5 Variation of energy and exergy efficiencies by varying the mass flow of feed water, in a mill with baghouse boiler, T_0 25 ºC, T_{water} 30 ºC
Source: Own elaboration

Graph 6 shows the variation of the energy and exergy efficiencies when the mass flow of the feed water is modified, keeping the dead state temperature (T_0) fixed at 25 ºC, and the inlet water temperature (T_{water}) at 90 ºC. We observe that the efficiencies increase as the mass flow rate increases, but the values achieved are lower with respect to the case of T_{water} at 30 ºC. The increase in energy efficiency is more noticeable with an increase of 49 units. However, as a point of comparison we take the mass flow of 21.5 kg/s, where it does not reach 74 units; on the other hand, the exergy efficiency, for 21.5 kg/s the change was negligible. It is more convenient to keep the supply water temperature at 30 ºC. It is clear that the mass flow rate of the inlet water is more important as a parameter to increase the overall efficiencies in the complete cycle of a plant than the temperature of the water.

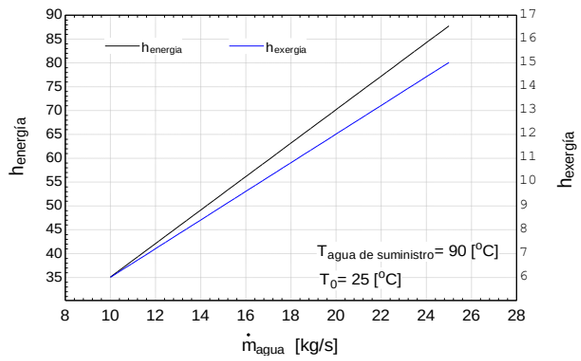

Graphic 6 Variation of energy and exergy efficiencies when varying the mass flow of feed water, in a mill with baghouse boiler, T_0 25 ºC, T_{water} 90 ºC
Source: Own elaboration

Graph 7 shows the variations of the energy and exergy efficiencies when the dead state temperatures are modified, keeping the feed water mass flow rate fixed at 21.5 kg/s and the inlet water temperature (T_{water}) at 30 ºC to compare how the efficiencies change when the dead state temperature is modified. For this case it is observed that the exergy efficiency increases as the dead state temperature decreases, going from 25.8 units (at 40 ºC) to 28.5 (at 16 ºC). The gain is small, but it increases. It is concluded that the process is more efficient in the autumn-winter season (when the ambient temperature is between 20 to 23 ºC) in Campeche. It is observed that the energy efficiency remains constant at a value just below 74 units. This efficiency is not affected by the ambient temperature. It can be understood because in the corresponding equation the temperature variable of the dead state is not involved. Unlike the exergy efficiency equation where it is present in the entropy generation term; equations 1 to 16.

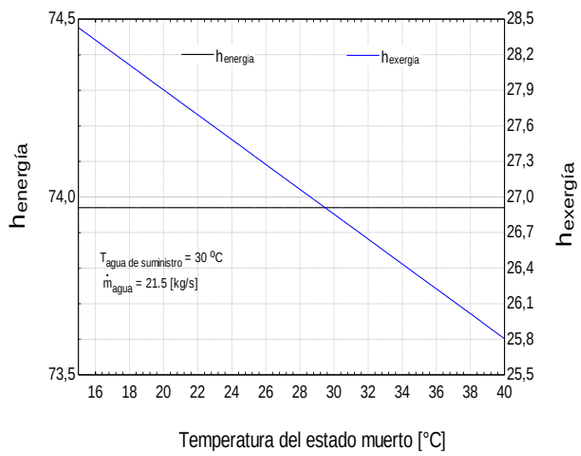

Graphic 7 Variation of the energy and exergy efficiencies by modifying the dead state temperatures and keeping fixed the generator water inlet temperature (T_{water}) 30ºC, and the mass flow of feed water at 21.5 kg/s.
Source: Own elaboration

ISSN-2523-2517

In Figure 8, to compensate a little for the null effect of the dead state temperature variation on the exergy efficiency (Figure 6), the variation of the energy and exergy efficiencies was made by including a variable called water temperature (T_{water}) obtained by subtracting a constant of 3 ºC from the dead state temperature (T_{water} = [Dead test -3] ºC) to reach the wet bulb temperature of the water, in such a way that it affects the thermodynamic temperatures involved in the energy efficiency equation. Keeping the feedwater mass flow rate and inlet water temperature fixed. For this case it is observed that the exergy efficiency increases as the dead state temperature decreases, going from 25.6 units at 40 ºC, to 28.5 units at 15 ºC. On the other hand, the energy efficiency also increases from 73.3 units at 40 ºC to 75.6 units at 15 ºC. As in Graph 5, it is concluded that the process is more efficient in the autumn-winter season, when the ambient temperature decreases in Campeche. Equations 1 to 16 were also used, but the thermodynamic changes that occur when the inlet water temperatures are modified are taken into account; this is a more realistic situation due to the relationship of water temperature with the environment.

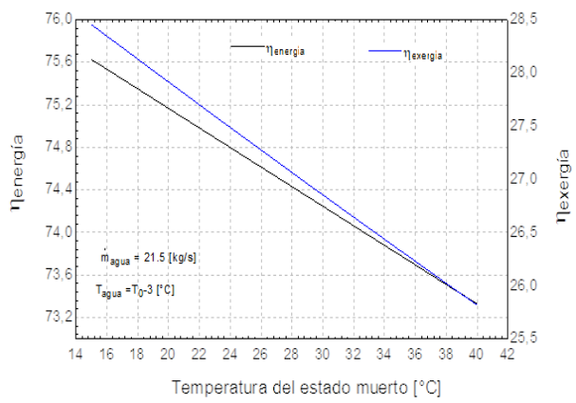

Graphic 8 Variation of energy and exergy efficiencies by modifying the dead state temperatures while maintaining the generator water inlet temperature, $T_{water} = T_{0\text{-}3}$ ºC, and the feed water mass flow rate at 21.5 kg/s
Source: Own elaboration

Conclusions

A baghouse boiler was modeled in 1st and 2nd law of thermodynamics, as well as the complete cycle of the sugar mill "La Joya" in the state of Campeche, Mexico. For the mathematical modeling, the equations reported in the literature were used. The combustion chamber is the area where the greatest exergy loss is concentrated.

In this area, losses of 68% of the fuel input exergy are considered (Singh, 2019). It should be noted, that for the operation of this boiler the fuel (bagasse) is not necessary to save it. It is more necessary is to decrease the consumption of feed water because of the cost associated with the extraction, water treatment, as well as the care of the quality of the steam produced by the boiler. From the behavior of the model, it is clear that a lower ambient temperature results in a lower exergy destruction and therefore in a higher second law efficiency. From the boiler analysis, the following conclusions can be drawn:

– Energetic Analysis; the optimum values for the operation of the electric generation system were determined.

– Energetic analysis; the parametric analysis of the exergy destroyed in the boiler was carried out, observing the factors that have the greatest influence on the generation of entropy.

The variables considered were:

- Inlet water temperature.
- Mass flow rate.
- Dead state temperature.

– Simulations were carried out to determine the energy and exegetic efficiencies of the steam generator with the Engineering Equation Solver Software (EES).

– According to Graphs 5 and 6, the efficiency of the boiler is affected according to the time of the year; that is, at the beginning of the harvest, when the dead state temperature is (T_0) 20ºC, there is a maximum efficiency with respect to the dead state temperature in the hottest seasons.

ISSN-2523-2517

- The steam mass flow required for the boiler was determined to be 16.6 kg/s, which is equivalent to a saving of 5 kg/s with respect to the mass flow with which the plant was operating (21.5 kg/s). The boiler was more efficient in controlling the mass flow of water, saving treated water consumption and meeting the goal of obtaining the steam necessary for the process with the least destruction of exergy. In addition, there is a smaller amount of softened water, which reduces operating costs.

- In the separate exergy analysis of the boiler, an increase in the feed water temperature produces a lower exergy destruction in the boiler; but when considering this same parameter in the overall exergy efficiency of the cycle, it results in a lower efficiency.

- The behavior of the sugar mill as a whole was determined to establish the feasibility of controlling or not, the mass flows of the feed water, as well as its inlet temperature.

- By modifying the mass flow of the feed water and keeping the dead state temperature (T_0) fixed at 25 ^oC, and the inlet water temperature (T_{water}) at 90 ^oC, to compare how the efficiencies change, it was observed that they increase as the mass flow increases; by increasing the mass flow from 10 to 25 kg/s and with T_{water} at 90 ^oC, there was an increase of 53 units in the energy efficiency, reaching a maximum of 88 units.

- For T_{water} at 90 ^oC, the energy efficiency changed by 9 units from 6 to 15 units. It was concluded that, it is much more important to increase the mass flow of the inlet water to increase the overall efficiencies in the installations of a mill, than the temperature of the same.

- Variations in energy and exergy efficiencies were determined by varying the dead state temperatures, keeping the feedwater mass flow rate and inlet water temperature fixed. It was observed that the exergy efficiency increases with decreasing dead state temperature. It is concluded that the process is more efficient in the autumn-winter season, when the ambient temperature decreases in Campeche. On the other hand, it is observed that the energy efficiency remains constant at a value slightly lower than 74 units. This efficiency is not affected by the ambient temperature. It is understood because in the corresponding equation the temperature variable of the dead state is not involved. Unlike the exergy efficiency equation where it is present in the entropy generation term.

- To compensate for the null effect of the T0 variation in the exergy efficiency, the water temperature variable (Tagua) was included with a constant of 3 ^oC (Twater = [Dead Tested -3] ^oC to simulate the wet bulb temperature; in such a way that it affects the temperatures involved in the energy efficiency equation. Feedwater mass flow rate and inlet water temperature were kept fixed. It was observed that the exergy efficiency increased as the dead state temperature decreased from 25.6 units at 40 ^oC to 28.5 units at 15 ^oC. The energy efficiency also increased from 73.3 units at 40 ^oC to 75.6 units at 15 ^oC.

References

Cengel, Y. A. (2011). *Transferencia de Calor y Masa* (S. A. D. C. V. McGRAW-HILL/INTERAMERICANA EDITORES (ed.); Cuarta edi). ISBN 978-607-15-0540-8.

Cengel, Y. A. (2015). *Termodinámica* (S. A. D. C. V. McGRAW-HILL/INTERAMERICANA EDITORES (ed.); 8a ed. ISBN 978-607-15-1281-9

Hugot, E. (2011). Manual Del Ingeniero Azucarero. In *El café en Colombia, 1850-1970*. https://doi.org/10.2307/j.ctv47w55p.5

ISSN-2523-2517

Kanoglu, M., & Dincer, I. (2009). Performance assessment of cogeneration plants. *Energy Conversion and Management*, *50*(1), 76–81. https://doi.org/10.1016/j.enconman.2008.08.029

Ma, Z., Zhang, K., Xiang, H., Gu, J., Yang, M., & Deng, K. (2023). Experimental study on influence of high exhaust backpressure on diesel engine performance via energy and exergy analysis. *Energy*, *263*, 125788. https://doi.org/10.1016/J.ENERGY.2022.125788

Manso, W. y Castillo, C. (2015). Calderas de Ingenios Azucareros. Retos y Soluciones. *Revista ATAM, Edit. Asociación de Técnicos Azucareros de México A.C*, *26*, 17.

Molina López, D. L. (2015). *Modelación matemática basada en análisis exergético de una caldera bagacera* (Issue 1). UNIVERSIDAD AUTÓNOMA DE OCCIDENTE.

Pistore, T. (2012). Estudios de casos de sistemas de cogeraçao. In *Curso Internacional sobre Energía na industria açucar e alcohol*.

Ramos, V. F., Pinheiro, O. S., Ferreira da Costa, E., & Souza da Costa, A. O. (2019). A method for exergetic analysis of a real kraft biomass boiler. *Energy*, *183*, 946–957. https://doi.org/https://doi.org/10.1016/j.energy.2019.07.001

Rivero, R. y Anaya, A. (1986). El método de exergía: sistemas energéticos económicos y eficientes. *Seminario de Aplicaciones Factibles de Conservación y Ahorro de Energía En Fase de Proyecto.*, 12.

Ruiz Labourdette, C. M. (2012). *ANÁLISIS ENERGETICO DE CALDERA BAGACERAMARCA BABCOCK & WILCOX: PROPUESTA DEINSTALACIÓN DE ECONOMIZADOR No Title*. Universidad Veracruzana.

Singh, O. K. (2019). Exergy analysis of a grid-connected bagasse-based cogeneration plant of sugar factory and exhaust heat utilization for running a cold storage. *Renewable Energy*, *143*, 149–163. https://doi.org/10.1016/j.renene.2019.05.012

Thomasset, C. W. (2011). Pequeño manual del foguista. *Manual Del Foguista*, *10*, 439.

Tornero, F. (2011). Producción de vapor en ingenios azucareros. Prácticas de Seguridad en el Sector Agroindustrial. STPS 1. *Dirección General de Seguridad y Salud En El Trabajo (D.G.S.S.T).*, 20.

Vallejo, E. V. J. (1982). El concepto de exergia y su aplicacion a la industria azucareraNo Title. In *Estacion Experimental Agro-Industrial*, (Vol. 137, p. 50).

ISSN-2523-2517

Article **Journal Electrical Engineering**
December 2023, Vol.7 No.19 38-42

Evaluation of the adherence of thermoplastic polyurethane (TPU) as an alternative material for the protection of solar cells

Evaluación de la adherencia del poliuretano termoplástico (TPU) como material alternativo de protección de celdas solares

SALAZAR-PERALTA, Araceli´†*, PICHARDO-SALAZAR, José Alfredo´´, PICHARDO-SALAZAR, Ulises´´´ and BERNAL-MARTÍNEZ, Lina´

´*TecNM: Tecnológico de Estudios Superiores de Jocotitlán, Carretera Toluca Atlacomulco km 44.8, Ejido de San Juan y San Agustín, Jocotitlán, México.*
´´*Centro de Bachillerato Tecnológico Industrial y de Servicios No. 161, Ex hacienda la Laguna S/N Barrio de Jesús 2a Sección, San Pablo Autopan, Toluca. Estado de México*
´´´*Centro de Estudios Tecnológicos Industrial y de Servicios no. 23. Avenida, Del Parque s/n, 52000 Lerma de Villada, México.*

ID 1st Author: *Araceli, Salazar-Peralta* / **ORC ID:** 0000-0001-5861-3748, **Researcher ID Thomson:** U-2933-2018, **CVU CONAHCYT ID:** 30 0357

ID 1st Co-author: *José Alfredo, Pichardo-Salazar* / **ORC ID:** 0000-0002-8939-9921

ID 2nd Co-author: *Ulises, Pichardo-Salazar* / **ORC ID:** 0000-0002-3758-2038

ID 3rd Co-author: *Lina, Bernal-Martínez* / **ORC ID:** 0000-0002-4922-043X

DOI: 10.35429/JEE.2023.19.7.38.42 Received July 30, 2023; Accepted December 30, 2023

Abstract

At present, the care of the environment as well as the use of solar energy are of great importance. One way to use solar energy for clean energy generation is through the use of photovoltaic modules. The performance of the crystalline silicon PV module is mainly determined by the efficiency of the silicon cells, but the properties of the other components, such as the encapsulant material, also have a high impact. The objective of this study was to evaluate the adherence of Thermoplastic Polyurethane (TPU) as an alternative material for the protection of solar cells, since the encapsulating material most used in solar production to date is Ethylene vinyl acetate (EVA) and it serves as a comparison of possible advantages and disadvantages. The tests carried out were in accordance with the International IEC 61215 and 61345 Standards. The adhesion results were sufficiently good and without optical defects. It is concluded that TPU can be used as an alternative material for encapsulating solar cells.

Photovoltaic module, Encapsulating material (EVA, TPU), Solar cell

Resumen

Actualmente el cuidado del medio ambiente así como el aprovechamiento de la energía solar son de gran importancia. Una manera de utilizar la energía solar para la generación de energía limpia es por medio del uso de módulos fotovoltaicos. El rendimiento del módulo fotovoltaico de silicio cristalino está determinado principalmente por la eficiencia de las células de silicio, pero las propiedades de los otros componentes, como el material encapsulante, también tiene un alto impacto. El objetivo de este estudio fue evaluar la adherencia del Poliuretano Termoplástico (TPU) como un material alternativo para la protección de celdas solares, ya que el material encapsulante más utilizado en la producción solar hasta la fecha es el Etilen vinil acetato (EVA) y sirve como comparación de posibles ventajas y desventajas. Las pruebas realizadas fueron conforme a las Normas Internacionales IEC 61215 y 61345. Los resultados de adherencia fueron suficientemente buenos y sin defectos ópticos. Se concluye que el TPU se puede utilizar como material alternativo para el encapsulado de celdas solares.

Módulo Fotovoltaico, Material encapsulante (EVA, TPU), Celda solar

Citation: SALAZAR-PERALTA, Araceli, PICHARDO-SALAZAR, José Alfredo, PICHARDO-SALAZAR, Ulises and BERNAL-MARTÍNEZ, Lina. Evaluation of the adherence of thermoplastic polyurethane (TPU) as an alternative material for the protection of solar cells. Journal Electrical Engineering. 2023. 7-19:38-42.

* Correspondence to Author (E-mail: araceli.salazar@tesjo.edu.mx)
† Researcher contributing as first author.

Introduction

Polyurethanes are polymers that contain urethane groups in the molecular chain, and specifically, thermoplastic polyurethanes are made up of linear block copolymers in which rigid segments alternate, formed by a diisocyanate and a chain extender, and flexible, formed by macrodiols. Sometimes they can be formed by different types of molecules that make them have different energies and ways of interacting between the polymer chains and form a material with specific properties [1, 2, 3].

Urethane thermoplastic elastomers. They are block copolymers and are formed by polyaddition of long-chain organic compounds, the so-called diols. TPUs offer very good processing options due to a mix of hard and soft meltable segments. In polyaddition, short-chain glycols that react with diisocyanates (hard molecule segments) and long-chain polyesters or polyethers that react with diisocyanates (soft molecule segments) are mixed in a suitable ratio [2]. Different mixing ratios of soft and hard segments result in materials with different levels of hardness, but nevertheless elastic [4].

Function of the protective material

Nowadays, the shielding material is one of the most important components of a solar module today and must meet many requirements [5, 6, 7]. It is mainly used to bond and encapsulate solar cells and is intended to protect them from the effects of weather in the long term. The protective materials used must have the best possible resistance against water vapor and oxygen, otherwise the metal contacts and interconnections can corrode and as a result the solar module becomes unusable. The inclusion material can also be damaged by excess oxygen or water vapor absorption, whereby it turns yellow and therefore causes a loss of transmission. A high degree of transmission of light is very important for the materials used, since the transmission of the material is directly related to the generation of electricity. The higher the transmission of a material, the more light the cell can absorb and convert it into electricity [8, 9].

Furthermore, a good embedding material should have relatively high heat resistance on the one hand and good thermal conductivity on the other, as the modules can heat up to 90 degrees in direct sunlight [10, 11]. Materials have this so-called blur or string slippage when the embedding material softens at higher temperatures. When the embedding material softens at higher temperatures or liquefies it can no longer provide the necessary support. The better the thermal conductivity of the encapsulation materials, the better the heat can be dissipated and the higher the performance that can be achieved [12]. The embedding material also ensures that the module remains stable and serves as protection in the event of glass breakage. The materials used must, among other things, have a high level of stability against UV radiation, since shortwave radiation can yellow the material and cause transmission losses [13]. Due to the different incorporated materials with different coefficients of thermal expansion, the embedding material must compensate for the stresses that occur so that they do not cause cell ruptures or damage to the module. All the properties listed here must be fulfilled by a good material so that durable and efficient modules can be produced.

Methodology to develop

This study was carried out as follows. Conforms to International Standards IEC 61215 and 61345.

- 200 x 200 mm samples of the encapsulating material TPU were taken, as well as 200 x 200 mm samples of the encapsulating material EVA (Ethylene Vinyl Acetate).
- The samples were rolled in the Spire Brand Laminator. Figure 1.
- The lamination conditions were the following: Temperature 150°C ± 3°C. evacuation time (vacuum) of 210 seconds, and a pressure time at 800mbar of 360 seconds.
- Twelve laminated samples of each encapsulating material, were placed in the Temperature/Humidity climatic chamber with the following conditions: 1000 h at 85°C ± 2°C and relative humidity of 85 ± 5%.

ISSN-2523-2517

- Twelve laminated samples of each encapsulating material, were submitted in a chamber for Ultraviolet tests with the following test conditions: 1000 h and irradiation of 15kWh/m^2.

- The measurement of the adhesion was carried out after the laminate with a dynamometer for manual use. Figure 2. With a capacity of 50N, applying tensile force with an angle of 180° for maximum load application.

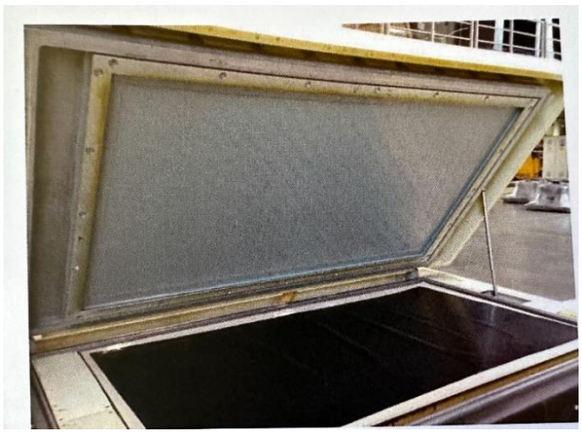

Figure 1 Laminator marca Spire
Source: Own elaboration

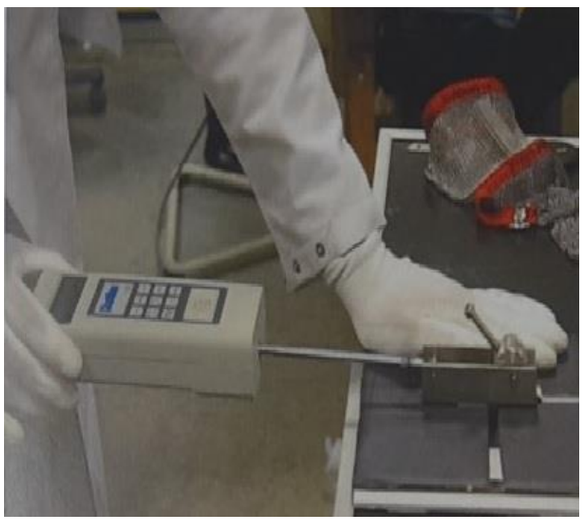

Figure 2 Adhesion test Dynamometer
Source: Own elaboration

Results

After the tests the results obtained were the following:

- As can be seen in Table 1. The values of resistance to adhesion of the EVA material, as well as those obtained from the TPU material, comply with the specification established in the Standard (25N minimum). After aging in a climatic chamber with (1000 h at 85°C ± 2°C and relative humidity of 85 ± 5%), the Eva presented adherence values of 25 to 40 N/cm. On the other hand, the TPU withstood more than 50N/cm.

Sample number	EVA N/cm	TPU N/cm
1	30	> 50
2	25	> 50
3	25	> 50
4	40	> 50
5	40	> 50
6	40	> 50
7	35	> 50
8	35	> 50
9	36	> 50
10	36	> 50
11	37	> 50
12	38	> 50

Table 1 Resistance to adhesion in N/cm of EVA and TPU after aging in a climatic chamber (temperature and humidity)
Source: Own elaboration

- After the aging test in a UV chamber (1000h) with irradiation of 15kWh/ and a temperature of 60°C±3°C, the values obtained with the EVA were: 40 to 50 N/cm, instead the values obtained with the TPU they were greater than 50N. Table 2.

Sample number	EVA N/cm	TPU N/cm
1	40	> 50
2	40	> 50
3	45	> 50
4	50	> 50
5	50	> 50
6	45	> 50
7	50	> 50
8	46	> 50
9	48	> 50
10	49	> 50
11	49	> 50
12	50	> 50

Table 2 Resistance to adhesion of EVA and TPU in N/cm after 1000h in a UV chamber
Source: Own elaboration.

Acknowledgments

To Jehovah God who provides health and understanding to be able to do research

ISSN-2523-2517

To the Tecnológico Nacional de México, to which the Tecnológico de Estudios Superiores de Jocotitlán belongs, for its scientific and moral Support.

To the Tecnológico de Estudios Superiores de Jocotitlán for the support with the Research hours provided. And the Center of Academy-Industry Linkage.

To all my collaborators who with their support make teamwork possible. to carry out these studies.

Conclusions

The adhesion test measures the resistance between the individual materials and is given in N/cm.

In all tests, the adhesion must not be less than 25 N/cm and must be distributed as evenly as possible throughout the laminate. The adhesion of the embedding materials must have, on the one hand, good adhesion to glass and, on the other hand, guarantee good adhesion properties to the carrier films. There are some differences in the chemical structure and surface treatment of the backsheets, which have a great influence on the adhesion to the inlay material.

In this study, the adherence results obtained in a comparative way of the 2 materials EVA and TPU can be observed after having been submitted in a humidity and temperature climatic chamber (1000 h at 85°C ± 2°C and relative humidity of 85 ± 5%), according to the results it can be deduced that the adhesion resistance of TPU is higher than that of the EVA material currently used.

According to the results obtained after the test in a UV chamber with an irradiation of 15kWh/m2, and a temperature of 60°C±3°C, it is also observed that the adhesion resistance values of the TPU exceed the resistance values of EVA.

In this test, the focus was on the adhesion of the inlay material. good enough and without optical defects for the 2 materials EVA and TPU.

It is concluded that the encapsulating material TPU is an alternative option to be used in the encapsulation of solar panels.

References

[1] A. Gabor, M. Ralli, S. Montminy, L. Alegria, C. Bordonaro, J. Woods, L. Felton, ”Soldering induced damage to thin Si solar cells and detection of cracked cells in modules, *Proceedings of the 21st EUPVSEC*, Dresden, Ger-many, 2006, pp. 2042– 2047. Steelandsilicon.com https://steelandsilicon.com/pubs/Gabor_20060914

[2] A. W. Czanderna and F. J. Pern, Encapsulation of PV modules using ethylene vinyl acetate copolymer as a pottant: a critical review, Solar Energy Material and Solar Cells, vol. 43, pp.101-181, 1996. https://www.osti.gov/etdeweb/biblio/378259
DOI: https://doi.org/10.1016/0927-0248(95)00150-6

[3] Barrera, P. (2009). ”Simulación y caracterización de celdas solares multi-juntura y de silicio cristalino para aplicaciones espaciales.´´ (Tesis de Doctorado). Universidad Nacional de General San Martin Comisión Nacional de Energía Atómica Instituto de Tecnología. República Argentina. https://www.tandar.cnea.gov.ar/doctorado/Tesis/Barrera.pdf

[4] Baur, Brinkmann, Osswald, Schmachtenberg: Saechtling Kunststoff Taschenbuch; Hanser Verlag; 2007. https://www.hanser-elibrary.com/doi/book/10.3139/9783446414372

[5] B.Ketola, K. R. McIntosh, A. Norris, ad M. K. Tomalia, Silicones for photovoltaic encapsulation: In: Proceedings of the 23rd European Photovoltaic Solar Energy Conference and Exhibition, Feria Valencia, Spain, pp. 2969-2973, WIP-Munich, 2008. https://www.researchgate.net/publication/266496217_Silicones_for_Photovoltaic_Encapsulation

[6] BGI Research, Ethylene vinyl acetate (EVA) global market to 2015 - photovoltaic encapsulants to drive EVA demand in the future, 2011. https://www.jinjichemical.com jinjichemical.com

[7] G. Oreski and G. M. Wallner, Aging mechanisms of polymeric films for PV encapsulation, Solar Energy, vol. 79, pp. 612-617, 2005. https://www.scirp.org/(S(351jmbntvnsjt1aadkposzje))/reference/referencespapers.aspx?referenceid=1662930 Cirp.org.

[8] H. Schmidhuber and K. Krannich, Why using EVA for module encapsulant if there is a much better choice? In: Proceeding of the17th European Photovoltaic Solar Energy Conference, Munich, Germany, pp. 662-663, 2001. https://www.hindawi.com/journals/ijp/2007/027610/ https://doi.org/10.1155/2007/27610

[9] I. Kunze, S. Kajari-Schröder, X. Breitenmoser, B. Bjørneklett, ”Quantifying the risk of power loss in PV modules due to micro cracks,´´ Solar Energy Materials and Solar Cells 95, 2011, pp. 1131-1137. http://www.eupvsec-proceedings.com/proceedings?paper=7558

[10] Manuel Fernàndez Barrera. (2010). Energìa Solar: Energìa Fotovoltaica. Madrid: Liberfactory. https://es.scribd.com/document/508697594/energia-fotovoltaica

[11] Nada es para siempre: Química de la Degradación de Materiales R. M. Carranza, G. S. Dulfo y S. B. Farina. Instituto Nacional de Educación Técnica, Ministerio de Educación, Buenos Aires (2010). https://www.cab.cnea.gov.ar/ieds/images/extras/hojitas_conocimiento/materiales/pag_25_26_duffo_degrad_mater.pdf

[12] M. Sander, S. Dietrich, M. Pander, M. Ebert, M. Karraß, R. Lippmann, M. Broddack and D. Wald, ”Influence of manufacturing processes and sub-sequent weathering on the occurrence of cell cracks in PV modules,´´ Pro-ceedings of the 28th EUPVSEC, Paris, France, 2013, pp. 3275-3279. https://www.researchgate.net/profile/Mathias-Pander/publication/260054072_Influence_of_Manufacturing_Processes_and_Subsequent_Weathering_on_the_Occurrence_of_Cell_Cracks_in_PV_Modules/links/581efb7c08ae12715af5fc49/Influence-of-Manufacturing-Processes-and-Subsequent-Weathering-on-the-Occurrence-of-Cell-Cracks-in-PV-Modules.pdf

[13] Walter Michaeli: Einfuhrung in die Kunststoffverarbeitung; Hanser Verlag; 2006. https://www.booklooker.de/B%C3%BCcher/Angebote/autor=Walter+Michaeli&titel=Einf%C3%BChrung+in+die+Kunststoffverarbeitung.

ISSN-2523-2517

[[Title in Times New Roman and Bold No. 14 in English and Spanish]

Surname (IN UPPERCASE), Name 1st Author†*, Surname (IN UPPERCASE), Name 1st Co-author, Surname (IN UPPERCASE), Name 2nd Co-author and Surname (IN UPPERCASE), Name 3rd Co-author

Institutional Affiliation of Author including Dependency (No.10 Times New Roman and Italic)

International Identification of Science - Technology and Innovation

ID 1st Author: (ORC ID - Researcher ID Thomson, arXiv Author ID - PubMed Author ID - Open ID) and CVU 1st author: (Scholar-PNPC or SNI-CONAHCYT) (No.10 Times New Roman)

ID 1st Co-author: (ORC ID - Researcher ID Thomson, arXiv Author ID - PubMed Author ID - Open ID) and CVU 1st co-author: (Scholar or SNI) (No.10 Times New Roman)

ID 2nd Co-author: (ORC ID - Researcher ID Thomson, arXiv Author ID - PubMed Author ID - Open ID) and CVU 2nd co-author: (Scholar or SNI) (No.10 Times New Roman)

ID 3rd Co-author: (ORC ID - Researcher ID Thomson, arXiv Author ID - PubMed Author ID - Open ID) and CVU 3rd co-author: (Scholar or SNI) (No.10 Times New Roman)

(Report Submission Date: Month, Day, and Year); Accepted (Insert date of Acceptance: Use Only ECORFAN)

Abstract (In English, 150-200 words)

Objectives
Methodology
Contribution

Abstract (In Spanish, 150-200 words)

Objectives
Methodology
Contribution

Keywords (In English)

Indicate 3 keywords in Times New Roman and Bold No. 10

Keywords (In Spanish)

Indicate 3 keywords in Times New Roman and Bold No. 10

Citation: Surname (IN UPPERCASE), Name 1st Author, Surname (IN UPPERCASE), Name 1st Co-author, Surname (IN UPPERCASE), Name 2nd Co-author and Surname (IN UPPERCASE), Name 3rd Co-author. Paper Title. Journal Electrical Engineering. Year 1-1: 1-11 [Times New Roman No.10]

* Correspondence to Author (example@example.org)
† Researcher contributing as first author.

Introduction

Text in Times New Roman No.12, single space.

General explanation of the subject and explain why it is important.

What is your added value with respect to other techniques?

Clearly focus each of its features

Clearly explain the problem to be solved and the central hypothesis.

Explanation of sections Article.

Development of headings and subheadings of the article with subsequent numbers

[Title No.12 in Times New Roman, single spaced and bold]

Products in development No.12 Times New Roman, single spaced.

Including graphs, figures and tables-Editable

In the article content any graphic, table and figure should be editable formats that can change size, type and number of letter, for the purposes of edition, these must be high quality, not pixelated and should be noticeable even reducing image scale.

[Indicating the title at the bottom with No.10 and Times New Roman Bold]

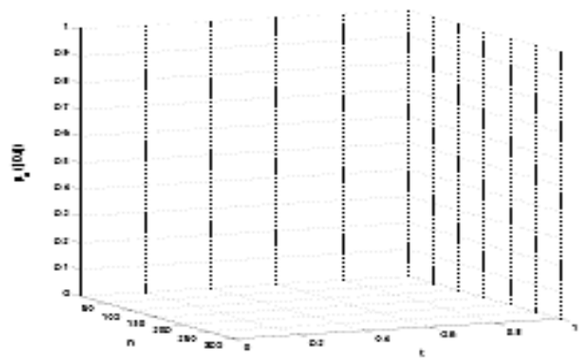

Graphic 1 Title and *Source (in italics)*

Should not be images-everything must be editable.

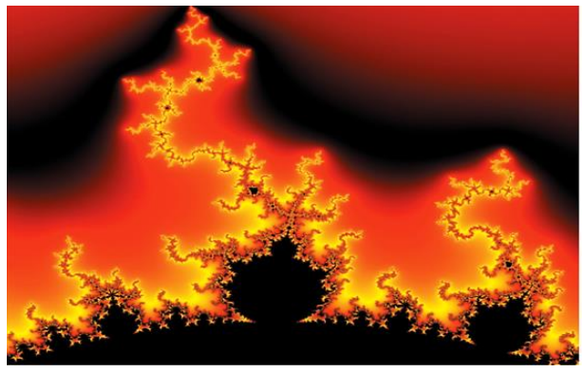

Figure 1 Title and *Source (in italics)*

Should not be images-everything must be editable.

Table 1 Title and *Source (in italics)*

Should not be images-everything must be editable.

Each article shall present separately in **3 folders**: a) Figures, b) Charts and c) Tables in .JPG format, indicating the number and sequential Bold Title.

For the use of equations, noted as follows:

$$Y_{ij} = \alpha + \sum_{h=1}^{r} \beta_h X_{hij} + u_j + e_{ij} \quad (1)$$

Must be editable and number aligned on the right side.

Methodology

Develop give the meaning of the variables in linear writing and important is the comparison of the used criteria.

Results

The results shall be by section of the article.

Annexes

Tables and adequate sources

Thanks

Indicate if they were financed by any institution, University or company.

ISSN 2523-2517

Conclusions

Explain clearly the results and possibilities of improvement.

References

Use APA system. Should not be numbered, nor with bullets, however if necessary numbering will be because reference or mention is made somewhere in the Article.

Use Roman Alphabet, all references you have used must be in the Roman Alphabet, even if you have quoted an Article, book in any of the official languages of the United Nations (English, French, German, Chinese, Russian, Portuguese, Italian, Spanish, Arabic), you must write the reference in Roman script and not in any of the official languages.

Technical Specifications

Each article must submit your dates into a Word document (.docx):

Journal Name
Article title
Abstract
Keywords
Article sections, for example:

1. Introduction
2. Description of the method
3. Analysis from the regression demand curve
4. Results
5. Thanks
6. Conclusions
7. References

Author Name (s)
Email Correspondence to Author
References

Intellectual Property Requirements for editing:

- Authentic Signature in Color of Originality Format Author and Coauthors.

- Authentic Signature in Color of the Acceptance Format of Author and Coauthors.

- Authentic Signature in blue colour of the Conflict of Interest Format of Author and Co-authors.

ISSN 2523-2517

Reservation to Editorial Policy

Journal Electrical Engineering reserves the right to make editorial changes required to adapt the Articles to the Editorial Policy of the Research Journal. Once the Article is accepted in its final version, the Research Journal will send the author the proofs for review. ECORFAN® will only accept the correction of errata and errors or omissions arising from the editing process of the Research Journal, reserving in full the copyrights and content dissemination. No deletions, substitutions or additions that alter the formation of the Article will be accepted.

Code of Ethics - Good Practices and Declaration of Solution to Editorial Conflicts

Declaration of Originality and unpublished character of the Article, of Authors, on the obtaining of data and interpretation of results, Acknowledgments, Conflict of interests, Assignment of rights and Distribution

The ECORFAN-Mexico, S.C. Management claims to Authors of Articles that its content must be original, unpublished and of Scientific, Technological and Innovation content to be submitted for evaluation.

The Authors signing the Article must be the same that have contributed to its conception, realization and development, as well as obtaining the data, interpreting the results, drafting and reviewing it. The Corresponding Author of the proposed Article will request the form that follows.

Article title:

– The sending of an Article to Journal Electrical Engineering emanates the commitment of the author not to submit it simultaneously to the consideration of other series publications for it must complement the Format of Originality for its Article, unless it is rejected by the Arbitration Committee, it may be withdrawn.

– None of the data presented in this article has been plagiarized or invented. The original data are clearly distinguished from those already published. And it is known of the test in PLAGSCAN if a level of plagiarism is detected Positive will not proceed to arbitrate.

– References are cited on which the information contained in the Article is based, as well as theories and data from other previously published Articles.

– The authors sign the Format of Authorization for their Article to be disseminated by means that ECORFAN-Mexico, S.C. In its Holding Republic of Peru considers pertinent for disclosure and diffusion of its Article its Rights of Work.

– Consent has been obtained from those who have contributed unpublished data obtained through verbal or written communication, and such communication and Authorship are adequately identified.

– The Author and Co-Authors who sign this work have participated in its planning, design and execution, as well as in the interpretation of the results. They also critically reviewed the paper, approved its final version and agreed with its publication.

– No signature responsible for the work has been omitted and the criteria of Scientific Authorization are satisfied.

– The results of this Article have been interpreted objectively. Any results contrary to the point of view of those who sign are exposed and discussed in the Article.

Copyright and Access

The publication of this Article supposes the transfer of the copyright to ECORFAN-Mexico, S.C. in its Holding Republic of Peru for its Journal Electrical Engineering, which reserves the right to distribute on the Web the published version of the Article and the making available of the Article in This format supposes for its Authors the fulfilment of what is established in the Law of Science and Technology of the United Mexican States, regarding the obligation to allow access to the results of Scientific Research.

Article Title:

Name and Surnames of the Contact Author and the Co-authors	Signature
1.	
2.	
3.	
4.	

Principles of Ethics and Declaration of Solution to Editorial Conflicts

Editor Responsibilities

The Publisher undertakes to guarantee the confidentiality of the evaluation process, it may not disclose to the Arbitrators the identity of the Authors, nor may it reveal the identity of the Arbitrators at any time.

The Editor assumes the responsibility to properly inform the Author of the stage of the editorial process in which the text is sent, as well as the resolutions of Double-Blind Review.

The Editor should evaluate manuscripts and their intellectual content without distinction of race, gender, sexual orientation, religious beliefs, ethnicity, nationality, or the political philosophy of the Authors.

The Editor and his editing team of ECORFAN® Holdings will not disclose any information about Articles submitted to anyone other than the corresponding Author.

The Editor should make fair and impartial decisions and ensure a fair Double-Blind Review.

Responsibilities of the Editorial Board

The description of the peer review processes is made known by the Editorial Board in order that the Authors know what the evaluation criteria are and will always be willing to justify any controversy in the evaluation process. In case of Plagiarism Detection to the Article the Committee notifies the Authors for Violation to the Right of Scientific, Technological and Innovation Authorization.

Responsibilities of the Arbitration Committee

The Arbitrators undertake to notify about any unethical conduct by the Authors and to indicate all the information that may be reason to reject the publication of the Articles. In addition, they must undertake to keep confidential information related to the Articles they evaluate.

Any manuscript received for your arbitration must be treated as confidential, should not be displayed or discussed with other experts, except with the permission of the Editor.

The Arbitrators must be conducted objectively, any personal criticism of the Author is inappropriate.

The Arbitrators must express their points of view with clarity and with valid arguments that contribute to the Scientific, Technological and Innovation of the Author.

The Arbitrators should not evaluate manuscripts in which they have conflicts of interest and have been notified to the Editor before submitting the Article for Double-Blind Review.

Responsibilities of the Authors

Authors must guarantee that their articles are the product of their original work and that the data has been obtained ethically.

Authors must ensure that they have not been previously published or that they are not considered in another serial publication.

Authors must strictly follow the rules for the publication of Defined Articles by the Editorial Board.

The authors have requested that the text in all its forms be an unethical editorial behavior and is unacceptable, consequently, any manuscript that incurs in plagiarism is eliminated and not considered for publication.

Authors should cite publications that have been influential in the nature of the Article submitted to arbitration.

Information services

Indexation - Bases and Repositories

LATINDEX (Scientific Journals of Latin America, Spain and Portugal)
EBSCO (Research Database - EBSCO Industries)
RESEARCH GATE (Germany)
GOOGLE SCHOLAR (Citation indices-Google)
MENDELEY (Bibliographic References Manager)
HISPANA (Information and Bibliographic Orientation-Spain)

Publishing Services

Citation and Index Identification H
Management of Originality Format and Authorization
Testing Article with PLAGSCAN
Article Evaluation
Certificate of Double-Blind Review
Article Edition
Web layout
Indexing and Repository
ArticleTranslation
Article Publication
Certificate of Article
Service Billing

Editorial Policy and Management

1047 La Raza Avenue - Santa Ana, Cusco - Peru. Phones: +52 1 55 6159 2296, +52 1 55 1260 0355, +52 1 55 6034 9181; Email: contact@ecorfan.org www.ecorfan.org

Journal Electrical Engineering

2523 2517
ISSN 2523-2517

www.ecorfan.org